



Semi-Annual Technical Report

July 1, 1970 - December 31, 1970

AD718878

Sponsored by

Advanced Research Projects Agency

ARPA Order No. 1644

Program Code Number POD10

Contractor: Stanford University

Contract No. DAHC15 70-G-12

Principal Investigators: D.A. Stevenson

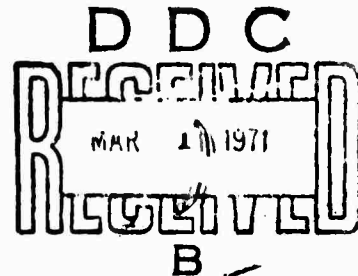
Phone : (415) 321-2300, Ext. 4251

R.H. Bube, Ext. 2535

G.S. Kino, Ext. 72289

W.D. Nix, Ext. 4259

W.A. Tiller, Ext. 2534



Grant Title: Synthesis of Compound Semiconducting Materials and Device Applications



CENTER FOR MATERIALS RESEARCH

STANFORD UNIVERSITY • STANFORD, CALIFORNIA

CMR 71-4

Reproduced by NATIONAL TECHNICAL INFORMATION SERVICE Springfield, Va. 22151

60

**BEST
AVAILABLE COPY**

Semi-Annual Technical Report

July 1, 1970 - December 31, 1970

Sponsored by

Advanced Research Projects Agency

ARPA Order No. 1644

Program Code Number POD10

Contractor: Stanford University

Contract No. DAHC15 70-G-12

Principal Investigators: D.A. Stevenson

Phone : (415) 321-2300, Ext. 4251

R.H. Bube, Ext. 2535

G.S. Kino, Ext. 72289

W.D. Nix, Ext. 4259

W.A. Tiller, Ext. 2534

**Grant Title: Synthesis of Compound Semiconducting Materials
and Device Applications**

Center for Materials Research

Stanford University

Stanford, California 94305

TABLE OF CONTENTS

I. INTRODUCTION	1
II. EPITAXIAL CRYSTAL GROWTH	2
III. APPLICATIONS OF COMPOUND SEMICONDUCTOR MATERIALS	10
IV. RELATIONS BETWEEN DISLOCATIONS AND MECHANICAL PROPERTIES AND THE PRODUCTION AND CHARACTERIZATION OF DEFECT STRUCTURE IN COMPOUND SEMICONDUCTORS	15
V. ANNEALING AND PRECIPITATION STUDIES IN COMPOUND SEMICONDUCTORS	21
VI. SCIENTIFIC ASPECTS OF SEMICONDUCTOR CRYSTAL PREPARATION	24

I. INTRODUCTION

The objective of this program is to improve the knowledge and state of the art concerning compound semiconducting materials with particular emphasis on their utilization in practical devices. The program consists of three principal sections: epitaxial crystal growth; device application; and fundamental materials studies. The epitaxial crystal growth section concerns the preparation of material suitable for the device applications. The major emphasis in device application is on microwave and acoustical devices utilizing thin film GaAs. The materials studies concern scientific aspects of crystal preparation and the properties of crystals of compound semiconductors. Since the focus of the program is directed towards the ultimate successful utilization of these materials, the specific systems selected for study are those showing outstanding promise for device applications, with the main emphasis on GaAs.

During the initial phase of the program, there has been significant progress on the preparation of thin films of GaAs using liquid phase epitaxial growth techniques. Initial problems concerning surface morphology and purity have been solved and wafers suitable for device fabrication are now being produced. With the recent availability of these wafers, studies of device applications are in their initial phases. In the materials studies, the initial activity has concerned the construction of relevant apparatus and the development of specific techniques required to approach each program. A description of research progress for the first six months of this program is given in the following report.

II. EPITAXIAL CRYSTAL GROWTH

A. PROGRAM OBJECTIVE

The epitaxial crystal growth effort is directed toward developing and evaluating liquid and vapor phase methods to prepare high quality layers of III-V semiconductors. The effort is also coordinated with the materials studies and device applications efforts to interact on mutual problems and to provide layers of specific dimensions and properties. To date, over 50 GaAs layers have been prepared on semi-insulating GaAs substrates by the liquid phase method to study the growth processes and to provide material for device applications. The initial objective has been achieved, i.e., to prepare high quality, uniform and reproducible layers of GaAs with n-type carrier densities in the mid 10^{14} cm^{-3} range, room temperature mobilities of $7000 \text{ cm}^2/\text{V-sec}$, and thicknesses in the $10 - 30 \text{ }\mu\text{m}$ range. At present, a study on the influence of temperature gradients on surface morphology is in progress, utilizing several different liquid phase processes. In addition, a vapor phase method of growth is to be developed to prepare layers with thicknesses in the $1 - 10 \text{ }\mu\text{m}$ range and with n^+n contacts.

B. PROGRESS

After an extensive survey of the literature and visits to leading industrial research laboratories involved with III-V semiconductors, the liquid phase method of growth for GaAs was chosen for the initial phase of the epitaxial crystal growth effort. This method appeared to yield the high quality material required for the initial device applications. Two liquid phase systems were developed that have produced 52 GaAs layers on semi-insulating GaAs substrates for growth studies. Ten of these layers were grown to meet the high quality and uniformity required for device applications -- carrier densities in the mid 10^{14} cm^{-3} range, mobilities around $7000 \text{ cm}^2/\text{V. sec}$, and thicknesses in the $10 \text{ to } 30 \text{ }\mu\text{m}$ range. To achieve this quality, ultra clean techniques were developed for all stages of the preparation of the films.

C. GROWTH METHODS

There are essentially two methods used to prepare thin films of epitaxial III-V semiconductors: (1) growth from a liquid phase,¹ e.g., GaAs is recrystallized on a substrate from an As saturated Ga solution; and (2) growth from a vapor phase,² e.g., Ga and As compounds are vaporized by one of several techniques and then allowed to react at a lower temperature on a GaAs substrate. There are many variations on these methods that were considered. To meet the immediate high quality thin film requirements for the device effort, the liquid phase method was chosen for the initial work. This method yields epitaxial layers with low background impurity levels because of the very low impurity distribution coefficients³ and the required systems are less prone to serious contamination. The vapor phase method does not have these advantages. It will be developed later to provide thin films with thicknesses less than 10 μm .

There are three variations on the liquid phase method that are being evaluated: 1) the horizontal tilt process, fig. II-1a; 2) a vertical cell process, fig. II-1b,; and 3) a steady state process, fig. II-1c. The first two are operational and the third will be evaluated in the vertical cell system.

A typical method of operation for the horizontal tilt system is as follows: a) a polycrystalline source of GaAs is placed at one end of a pyrolytic carbon boat and a specially prepared single crystal substrate of semi-insulating GaAs is placed at the other end; b) Ga is placed on the source and the boat is positioned in a scrupulously cleaned quartz tube at the center of the furnace; c) the quartz tube is evacuated and back filled with high purity hydrogen; d) the hydrogen is allowed to flow through the tube as the furnace heats to a saturation temperature; e) the liquid Ga is saturated with As from the source and then the furnace is tilted to allow the saturated Ga to roll onto the GaAs substrate; and f) the furnace is then cooled at a programmed rate to allow the GaAs to come out of solution and deposit on the GaAs substrate.

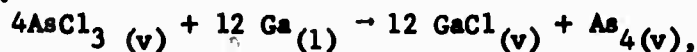
The operation of the vertical cell system is similar to the horizontal operation except that the source and substrate slices are placed normal to the axis of the cell and a temperature gradient is imposed along this axis. Initially the furnace is positioned such that the liquid Ga is saturated with

As on the GaAs source and then the furnace is rotated 180° to place the saturated Ga on the GaAs substrate. The temperature gradient is adjusted so that the temperature is a maximum between the source and substrate to prevent premature nucleation along the walls of the cell and on the surface of the saturated Ga.

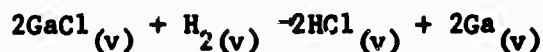
The steady state system will utilize the vertical cell system, but the operation will differ by 1) the temperature gradient will be as illustrated in fig. II-1c., 2) the source will be free to move in contact with the saturated Ga when the furnace is rotated 180°, and 3) the temperature at the GaAs substrate will remain constant during growth.

The vapor phase system will involve the following open tube process. A Ga source will be placed at one end of a 10 to 20°C/in temperature gradient in a furnace at 850° C. and the substrate will be placed at the other end at 750°C. High purity hydrogen will be fed through AsCl₃ at 20°C. to transport AsCl₃ vapor to the furnace. The significant reactions are the following:

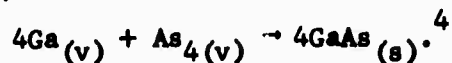
(1) 850°C.



@ 800°C.



and @ 750°C.



D. GROWTH VARIABLES

The growth variables in the liquid phase method are: 1) saturation temperature -- this controls the amount of GaAs that will come out of solution and deposit on the GaAs substrate, by virtue of the decreasing solubility of As in Ga with decreasing temperature; 2) cooling rate--this affects the interface stability and growth rate; 3) temperature gradient--same as 2); 4) substrate orientation--there are different growth rates in different directions, fig. IV-2, which underlie the influence of orientation on the surface morphology; and 5) As partial pressure--this influences nucleation on the substrate and minimizes evaporation of As from substrate prior to growth. The atmosphere surrounding the growth system, (H₂, O₂, etc.) is primarily responsible for the

formation and transport of impurities to and from the process. In addition to these growth variables, the surface preparation prior to crystal growth plays an important role, as discussed below.

E. SUBSTRATE PREPARATION

Considerable effort has been devoted to substrate preparation. The substrates, received as 20 mil thick slices, are first mechanically lapped and then either chem-mechanically or chemically polished. The chem-mechanical technique consists of polishing on a rotating Pellon pad with a 10:1 solution of deionized water to clorox. This method does not completely eliminate mechanical damage to the surface of the substrate. The chemical technique consists of rotating the substrate under a 16:1 solution of H_2SO_4 :30% solution of H_2O_2 . This technique needs further evaluation as it minimizes direct mechanical contact to the surface. Careful degreasing and cleaning procedures are also employed to minimize contamination on the surface and on the substrate as a whole before placing it in the furnace.

F. GROWTH RESULTS

The results obtained from 52 epitaxially grown GaAs thin films are summarized in Tables I and II. The layers all exhibit distinguishing surface morphologies that have some correlations with substrate growth defects, damage during preparation, orientation, cooling rate and mechanical agitation.

Figure II-3 shows the effect of dendritic growth around the edge of the substrate that arises from the fast growth rates in directions normal to the sides and edges of the substrate. The dendritic effect was virtually eliminated by the following modifications of the procedure: 1) a pyrolytic carbon mask was placed over the edges of the substrate so that the saturated Ga solution would only come in contact with the desired surface; and 2) increasing the cooling rate so that the rate of growth normal to the surface exceeded the transverse growth rates. Figures II-4a and b show the effect of using the mask and very fast cooling rates, respectively.

Terracing is the one general surface feature that overrides most of the layers produced. This effect can be controlled to a limited extent by changing the cooling rate and the surface orientation. Increasing the cooling rate

appears to decrease the size of the steps, fig. II-4, while orientation changes the general shape of the terraces, fig. II-5a and b. There is also some evidence that surface damage influences the width of the steps but this is not conclusive. In some cases the terracing did not appear at fast cooling rates but hillocks of several descriptions did appear, figs. II-6a, b and c. The shape of the hillocks does correlate with the surface orientation--triangular for the (111)A surface, hexagonal for the (111)B surface and rectangular for the (100)B surface. When the density of hillocks is large, they coalesce into a pattern that has the appearance of terracing, fig. II-6a-c. In some cases, however, large densities of hillocks also appear to form cellular growth patterns. Cellular growth arises from constitutional supercooling and a resultant interface instability.

There is some correlation of surface features with scratches and polishing marks on the surface of the substrate, fig. II-7. Microscopic observations of the substrates prior to growth, however, do not show the visual defects that have appeared after growth. These defects could arise at elevated temperatures from vaporization or sublimation of As in the vicinity of mechanical damage below the surface of the substrate. Increasing the partial pressure of As preceding growth may minimize this problem.

Improper cleaning and severe surface damage do contribute to incomplete nucleation and highly disarrayed terracing. Figure II-8a shows the effect of an acetone stain on the substrate. Figure II-8b shows the effect of air abrasion with 50 μm particles on the substrate surface.

G. ELECTRICAL PROPERTIES

Schottky barrier measurements and van der Pauw measurements have been made on a selected number of films grown. Since semi-insulating substrates are used, a special technique of analysis was developed for the Schottky barrier measurements. The technique employs a direct extrapolation of the net capacitance at an infinite bias voltage to find the shunting capacitance through the substrate. The results from this technique are shown in fig. II-9. With this technique the Schottky barrier and van der Pauw measurements are in excellent agreement. The results are summarized in Table I and II.

It is possible to achieve low 10^{14} cm^{-3} n-type carrier concentrations with the horizontal tilt process. The Ga has to be backdoped with Sn to obtain n-type material, as the undoped layers are of high resistivity and appear to be p-type. The Schottky barrier breakdown voltages are also quite large, $40 < V_b < 80$ volts. for Al electrodes.

H. UNIFORMITY

In general the layers are uniform in thickness and carrier concentration both to about 10% and reproducible under given growth conditions. Approximately 10 of the layers produced are suitable for device applications; however, the surface terracing must be eliminated to allow high resolution in photoetching processes, fig. II-10.

I. PROGRAM PLANS

The primary goal for the remainder of the year is to improve the surface quality of the epitaxial layers. This problem will be approached with continuing emphasis on substrate preparation and growth conditions. Handling techniques during lapping, polishing and cleaning of the substrates will be re-evaluated along with new polishing techniques such as r.f. sputtering. The study of the effects of growth rates at different substrate orientations, rates of cooling and temperature gradients will give considerable information on nucleation and stability of the liquid-solid interface. Careful measurements of the temperature profiles in the growth regions of each system will also elucidate some of the unknown growth conditions. These studies will be enhanced with the use of the newly installed scanning electron microscope to examine the surface features in detail.

Epitaxial growth by the liquid phase processes discussed above will be continued. The horizontal tilt process will be used to produce lower background impurity level layers that will have carrier concentrations in the 10^{13} cm^{-3} range. However, the surface morphology problems are likely to remain for some substrate orientations. The vertical cell and steady state processes will provide a means to study the influence of temperature gradients on surface morphology. Temperature gradients should localize and stabilize the growth kinetics at the solid-liquid interface.

Epitaxial growth by a vapor phase method will be used to grow layers thinner than 10 μm with smoother surface features. Initially, however, the background impurity levels are likely to be quite high because of the complexity of the system.

REFERENCES

1. H. Nelson, RCA Review 24, 603 (1963).
2. D. Effer and G.R. Antell, J. Electrochem. Soc. 107, 252 (1960).
3. R. Solomon, Proc. of Intern. Symp. GaAs, Dallas, 1968.
(Institute of Physics and the Physical Society, London).
4. J.F. Gibbons, P.C. Prehn, Report SEL-63-105 (Tr # 4711-1)
(Stanford Electronics Laboratories, Stanford, California. (Oct., 1963).
5. D.W. Shaw, IEEE Symposium on GaAs, 50 (1968).

TABLE I
GROWTH FROM HORIZONTAL TILT PROCESS

GROWTH NO.	$\frac{\mu(300^\circ\text{K})}{\mu(77^\circ\text{K})}$	CARRIER TYPE/ DENSITY	SUBSTRATE ORIENTATION	SATURATION TEMP. COOLING RATE	RESULTS AND COMMENT	CHANGES
29.			(111) - B	$\frac{750^\circ\text{C}}{15^\circ\text{C/hr.}}$	Smooth layer with light terracing, 2.0 mils thick. Sharp I-V breakdown.	Added additional S_n to melt for n-type material.
30.			(111) - B	$\frac{750^\circ\text{C}}{50^\circ\text{C/hr.}}$	Incomplete nucleation, hexagonal hillocks. Probably due to inadequate cleaning of substrate.	Increased cooling rate.
31.			(111) - B	$\frac{750^\circ\text{C}}{15^\circ\text{C/hr.}}$	Terraces with large dendritic growth along edges.	Normal cooling rate. Roughly lapped substrate with no subsequent polishing.
32.		n-type	(111) - B	$\frac{750^\circ\text{C}}{7^\circ\text{C/hr.}}$	Terraces surrounded by heavy dendritic growth.	Clean reactor tube. Improved substrate cleaning procedure with chem.-mechanical polish. Floating substrate. Reduced cooling rate.
33.			(111) - A	$\frac{750^\circ\text{C}}{-0^\circ\text{C/hr.}}$	Layer accidentally grown on roughly-lapped back side of substrate. Incomplete nucleation with many holes.	Floating substrate.
34.		n-type	(111) - B	$\frac{760^\circ\text{C}}{15^\circ\text{C/hr.}}$	Incomplete nucleation with petal-like terracing.	Chem.-mechanically polished substrate pitted with air-abrasive to increase nucleating sites. Submerged substrate. Clean reactor spade.
35.		n-type	(111) - B	$\frac{760^\circ\text{C}}{10^\circ\text{C/hr.}}$	Relatively good layer, 2.0 mils thick, with several minor flaws near the center. Light terracing.	Floating substrate.
36.		n-type	(111) - B	$\frac{760^\circ\text{C}}{10^\circ\text{C/hr.}}$	Good layer with light terracing.	Cleaned system. Submerged substrate.
37.			(100)	$\frac{750^\circ\text{C}}{10^\circ\text{C/hr.}}$	Overlapping, irregular terraces.	
38.		$2 \times 10^{14} \text{ cm}^{-3}$	(111) - B	$\frac{750^\circ\text{C}}{10^\circ\text{C/hr.}}$	Sharp/defined terraces, plateau in corner. No dendritic growth along edges of layer. Major improvement!	Used square "picture frame" carbon mask to prevent dendritic growth around edges.
39.		3×10^{14}	(111) - B	$\frac{760^\circ\text{C}}{10^\circ\text{C/hr.}}$	Very good layer with fine terracing. Plateau in corner.	Cleaned system. Used fresh charge of Ga. Substituted halocarbon grease for silicone grease in glass-glass seals.
40.		3×10^{14}	(111) - B	$\frac{650^\circ\text{C}}{10^\circ\text{C/hr.}}$	Light terracing. Carbon mask improperly aligned causing some dendritic growth along edge.	Reduced saturation temperature from 750°C to 650°C to reduce layer thickness

TABLE I (CONT'D)
GROTTES FROM HORIZONTAL TILT PROCESS

GROWTH NO.	$\mu(300^\circ\text{K})$ $\mu(77^\circ\text{K})$	CARRIER TYPE/ DENSITY	SUBSTRATE ORIENTATION	SATURATION TEMP. COOLING RATE	RESULTS AND COMMENT	CHANGES
41.		2×10^{15}	(111) - B	650°C 10°C/hr.	Medium terracing. Otherwise smooth layer, approximately 15 microns thick.	
42.	$\frac{5,800}{68,000}$	3×10^{14}	(100)	650°C 10°C/hr.	Smooth layer with fine terracing. Incomplete nucleation in local region - probably due to inadequate clearing.	
43.		p-type	(100)	750°C 10°C/hr.	Poor layer due to inadequate substrate preparation and movement of mask during initiation of growth.	Cleared system. Increased saturation temperature.
44.		p-type	(100)	750°C 10°C/hr.	Fine terracing with one significant plateau.	
45.		p-type	(100)	650°C 250°C/hr.	Excellent layer, very fine terracing, few pock marks.	Increased cooling rate to 250°C/hr.
46.		10^{15}	(111) - B	660°C 300°C/hr.	Excellent layer, smoother than #45.	Added S_{10} to Ga melt to produce n-type material. Increased cooling rate with fan.
47.	$\frac{7,200}{40,000}$	7×10^{14}	(100)	660°C 300°C/hr.	Good surface except for acetone stained region.	Changed clearing procedure (acetone as final rinse instead of isopropyl alcohol).
50.			(111) - B	660°C 300°C/hr.	Very irregular surface with overall etch-back.	No mask used.
52.	$\frac{6,300}{30,000}$	2×10^{15}	(111) - B	660°C 300°C/hr.	Uniform surface, fine terracing, no plateau.	System cleaned, baked out at 850°C , mask used.
53.			(100)	660°C 300°C/hr.	Closely packed square hillocks.	Specimen #45 reused as substrate.
55.			(100)	660°C 400°C/hr.	Closely packed rectangular hillocks. Some polishing scratches show through epi layer.	
56.			(111)	650°C 200°C/hr.	Irregular surface features.	Hand polished substrate on silk screen with 0.3 μ powder.

TABLE I (CONT'D)
GROWTH FROM HORIZONTAL TILT PROCESS

BLOCK NO.	$\frac{1000^2 \text{ cm}^2}{\text{min} \cdot \text{cm}^2}$	CARRIER TYPE/ DENSITY	SUBSTRATE ORIENTATION	SATURATION TEMP. COOLING RATE	RESULTS AND COMMENT	CHANGES
59.			(100)	$\frac{675^\circ\text{C}}{200^\circ\text{C/hr.}}$	Moderate, irregular terracing. Square hillocks in one corner.	
60.			(100)	$\frac{690^\circ\text{C}}{200^\circ\text{C/hr.}}$	Petal-like terracing. Polishing scratches show through epi layer.	
62.			(100)	$\frac{690^\circ\text{C}}{200^\circ\text{C/hr.}}$	Uniform surface, fine terracing. At high mag. fine protrusions can be seen all over surface particularly along terrace steps.	No mask used. Mechanically polished substrate.
63.			(111) - A	$\frac{690^\circ\text{C}}{250^\circ\text{C/hr.}}$	Isosceles triangular and connected triangular hillocks over perfectly smooth surface. All triangles are similarly oriented. Source rolled over with Ga.	Chem.-mechanically polished after band polishing on silk screen. No etching.
66.			(111) - A	$\frac{660^\circ\text{C}}{250^\circ\text{C/hr.}}$	Widely spaced flat terracing, very sharply defined. Scratches visible through layer. Source rolled over with Ga.	NO MASK used at 650° over week-end, 1 mg Sn added. NO MASK used
67.			(111) - A	$\frac{660^\circ\text{C}}{250^\circ\text{C/hr.}}$	Increased density of features as in #63. Source rolled over with Ga.	No etch. All fans and blowers shut down during growth, low vibration condition.
71.	$\frac{4,600}{14,000}$	3×10^{15}	(111) - A	$\frac{650^\circ\text{C}}{250^\circ\text{C/hr.}}$	Uniform, moderate terracing. Source rolled over with Ga.	Mask used. Etched in very weak Br for 20 min. Minor room vibration during growth.
73.			(111) - A	$\frac{660^\circ\text{C}}{250^\circ\text{C/hr.}}$	Triangular hillocks evenly spaced over surface.	System filled with H ₂ , but no H ₂ flow during growth. Chem.-mech. lapped by dripping method. No etch. No mask used. All fans and blowers off. Additional GaAs added to system to increase As partial pressure.
75.			(111) - A	$\frac{650^\circ\text{C}}{250^\circ\text{C/hr.}}$	Irregular triangular hillocks. Less densely scattered along one side of substrate.	Chem. polished with 16:1 H ₂ SO ₄ -H ₂ O ₂ after chem.-mech. lapping. 45 sec. etch in 2% Br-Methanol.
76.			(111) - B	$\frac{660^\circ\text{C}}{250^\circ\text{C/hr.}}$	Irregular terracing.	
77.			(111) - B	$\frac{660^\circ\text{C}}{250^\circ\text{C/hr.}}$	Similar to #76.	No crushed GaAs in spade. New source used. Room very quiet during growth period.

TABLE I (CONT'D)
GROWTH FROM HORIZONTAL TILT PROCESS

ROWTH NO.	$\mu(300^\circ\text{K})$ - (77°K)	CARRIER TYPE/ DENSITY	SUBSTRATE ORIENTATION	SATURATION TEMP. COOLING RATE	RESULTS AND COMMENTS	CHANGES
-8.			(111) - A	580°C 300°C/hr.	Very uniform, fine, irregular terracing with plateau near one corner.	
-9.			(111) - A	550°C 150°C/hr.	Off-center plateau with irregular terracing encircling it. Terraces become finer toward edge.	30 minute saturation period. Circular substrate used, no masking, no etch.

TABLE II
 PROFILES FROM VERTICAL CELL PROCESSES

SPOT NO.	$\mu(300^\circ \text{A})$ / $\mu(100^\circ \text{A})$	CARRIER TYPE/ DENSITY	SUBSTRATE OPERATION	SATURATION TEMP. /COOLING RATE	RESULTS AND COMMENT	REMARKS
46.			(100)	650°C 250°C/hr.	Rectangular hillocks. Possibly due to acetone residue on substrate surface.	System cleaned in standard manner prior to first growth.
49.		n-type	(111) - B	750°C 300°C/hr.	Sharply defined terraces and 2 plateaus. Some etch-back where clamped in holder.	Iso-propyl alcohol rinse, increased cooling rate.
51.	$\frac{5,300}{11,000}$	4×10^{16}	(100)	750°C 250°C/hr.	Fine terracing, one side very rough.	Post etched and crutch removed from salt. He heat sizzled used to increase temperature gradient near substrate interface.
54.			(111) - B	750°C 10°C/hr.	Fine and coarse terracing. Two large flaws in center. Cell contaminated due to temperature profiling.	Specimen #19 lapped off and reused as substrate.
57.			(111) - B	750°C 50°C/hr.	Some polishing scratches visible on substrate before loading. Smooth layer with fine, even terracing.	#32 lapped, cut, and reused as substrate. Chem.-Mech. lapped substrate.
58.			(100)	750°C 50°C/hr.	Fairly smooth layer with fine terracing accentuated in centre.	Kind polished substrate on silk screen. Terminated growth at 650°C .
61.			(111) - B	750°C 50°C/hr.	Moderate, irregular terracing.	Substrate mechanically polished on silk, no etch before growth.
64.			(111) - B	750°C 50°C/hr.	Moderate terracing.	Chem.-mechanically polished substrate with no chemical etch during preparation.
65.			(111) - B	750°C 50°C/hr.	Moderate terracing, very similar to #64.	
68.			(111) - A	750°C 50°C/hr.	Irregular terraces plus many scratch-like features paralleling substrate scratches.	
70.			(111) - A	750°C 250°C/hr.	Dense triangular hillock growth. Some lack of nucleation on substrate.	Removed considerable amount of substrate surface with long chem.-mechanical lap. Lightly etched with very dilute Br-methanol. Reduced system vibration to minimum.

TABLE II (CONT'D)
GROUHS FROM VERTICAL CELL PROCESS

TRIAL NO.	$\frac{u(300^\circ\text{K})}{u(700^\circ\text{K})}$	CARRIER TYPE/ DENSITY	SUBSTRATE ORIENTATION	SATURATION TEMP. COOLING RATE	RESULTS AND COMMENT	CHANGES
-2.			(111) - A	$\frac{750^\circ\text{C}}{50^\circ\text{C/hr.}}$	Petal-like terraces. Probably due to substrate contamination during cleaning procedure.	Slower cooling rate, otherwise repeat: 570.
-4.			(111) - A	$\frac{750^\circ\text{C}}{50^\circ\text{C/hr.}}$	Irregular terracing with noticeable randomness in a single central core area.	Terminate growth at 600°C.
50.			(111) - A	$\frac{750^\circ\text{C}}{50^\circ\text{C/hr.}}$	Large plateau surrounded by irregular terracing. Terracing becomes coarser towards edge.	Used chemical polish as final step (new procedure). Add additional heating coil to furnace to steepen temperature gradient in the region of the substrate interface.

Figure Captions

Figure II-1. Systems and temperature profiles in use for the liquid phase methods of growth: a) horizontal tilt system, b) vertical cell system, and c) steady state system. so and su indicate the source and substrate, respectively.

Figure II-2. Deposition rate versus crystallographic orientation on a (110) projection. The upper and lower halves of the polar diagram represent deposition on the Ga and As surfaces of the substrate, respectively. The diagram is symmetric about the [001]. (after Shaw, 5).

Figure II-3. This is an example of dendritic growth, growth No. 32, that arises from fast growth rates around the edges of the substrate. Note that the uneven surface features are terraces that have grown inwards from the dendrites. (111B, 8X)

Figure II-4. These growths show the results obtained by virtually eliminating dendritic growths around the edge of the substrate. (a) Growth No. 38 was masked around the edges of the substrate with a carbon frame so that the growth would be essentially normal to the surface. (111B, 8X) (b) Growth No. 62 was cooled at a faster rate so that the rate of growth normal to the surface would exceed transverse growth rates. Note that terracing occurs uniformly across the surface. (100, 8X)

Figure II-5. Typical micrographs of terracing that show (a) the ragged steps found on (111) A surfaces, growth No. 66 (50X), and (b) the smooth sharp edges found on (111)B surfaces, growth No. 38. (50X)

Figure II-6. These growths show typical hillock shapes found for particular substrate orientations. (a) Triangular hillocks are found on (111) A surfaces, growth No. 63. (10X) (b) Hexagonal hillocks are found on (111) B surfaces, growth No. 30. (8X) (c) Rectangular hillocks are found on (100) B surfaces, growth No. 48. Note that when the hillocks coalesce in large numbers, a terracing pattern appears to form. (10X)

Figure II-7. This growth shows a correlation of some surface features with possible defects inadvertently introduced during the preparation of the substrate. Some of the terraces and long lines appear to extend inwards from scratches observed on the masked portion of the substrate. (111A, 12X)

Figure II-8. These growths show features obtained when the substrate preparation was deliberately fouled. (a) The substrate was given a final rinse in acetone and a stain was left, growth No. 47. Note the propagation of the stain from the masked portion of the substrate into the growth. (100, 10X) (b) The substrate was air-abraded with 50 μm particles prior to growth, growth No. 34. Note the resultant irregular terracing and numerous holes. (111B, 8X)

Figure II-9. Carrier density determination from Schottky barrier capacitance and bias voltage measurements. The slope gives $n = 2 \times 10^{14} \text{ cm}^{-3}$ for growth No. 38. The capacitance for an infinite bias voltage has been subtracted from the measured capacitance. This corrects for the jig, substrate and edge shunt capacitances.

Figure II-10. Photodeposited F.E.T. networks on growth No. 47. (100, 10X)

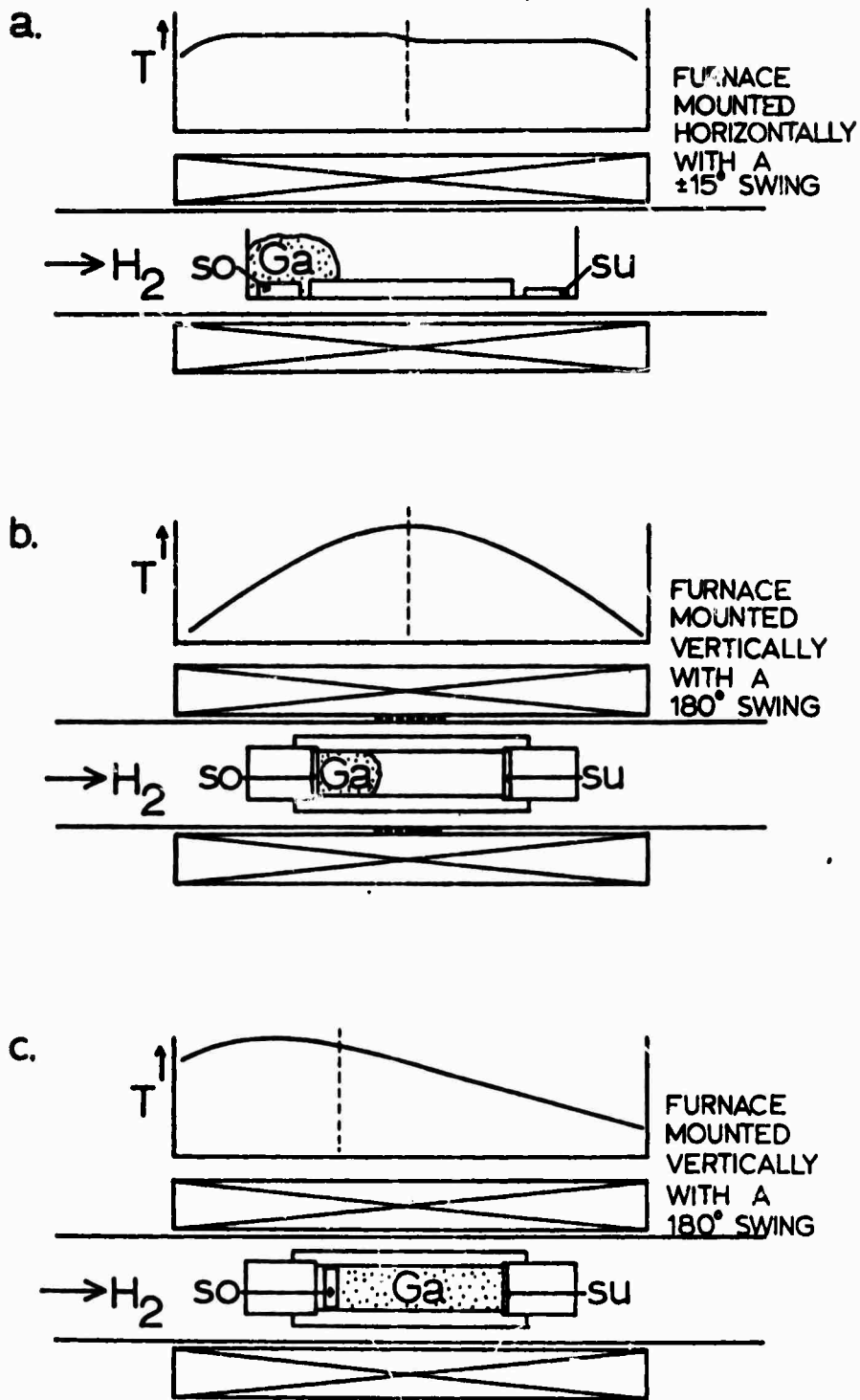


Figure II-1. Systems and temperature profiles in use for the liquid phase methods of growth: a) horizontal tilt system, b) vertical cell system, and c) steady state system. so and su indicate the source and substrate, respectively.

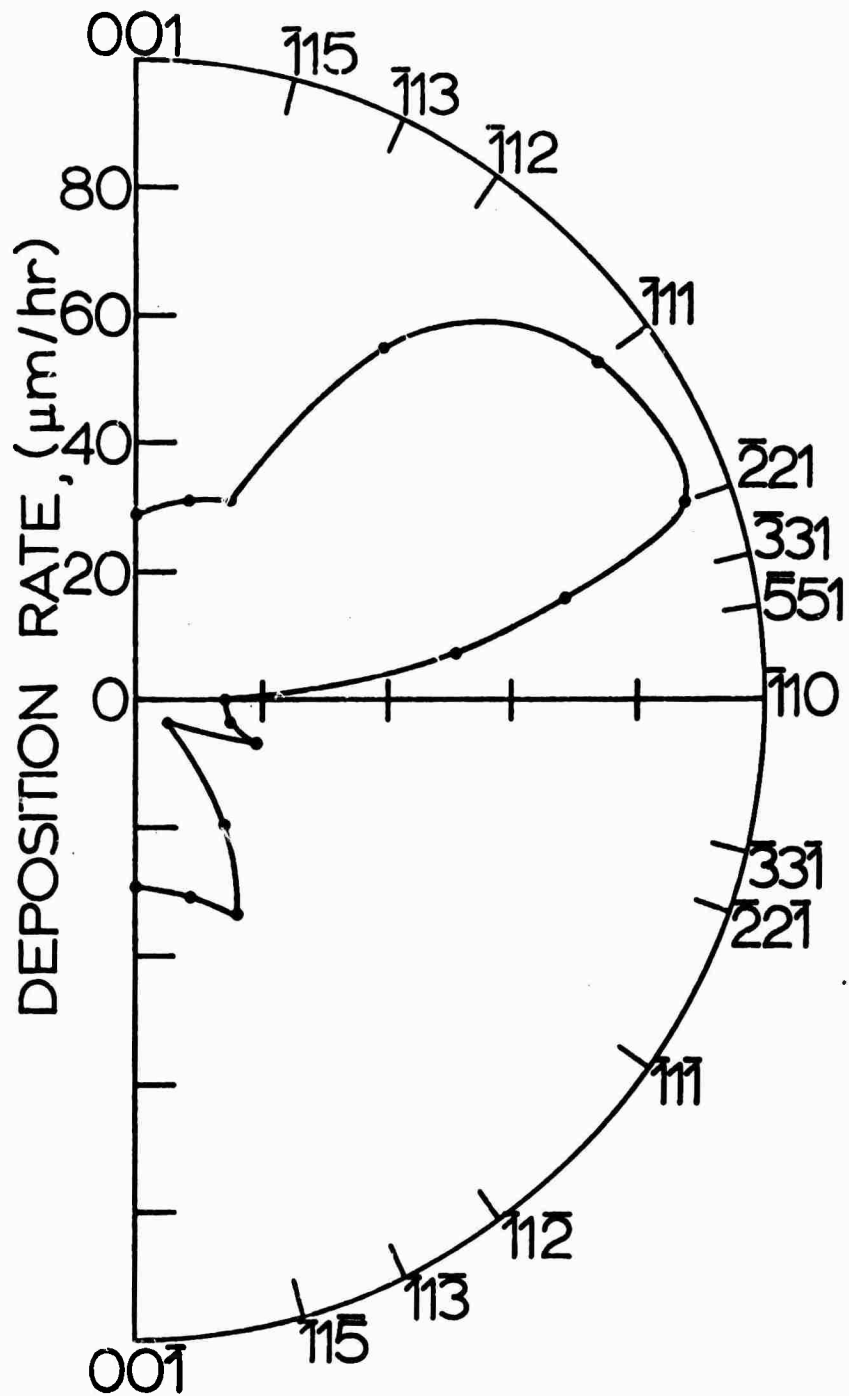


Figure II-2. Deposition rate versus crystallographic orientation on a (110) projection. The upper and lower halves of the polar diagram represent deposition on the Ga and As surfaces of the substrate, respectively. The diagram is symmetric about the $[001]$. (after Shaw.⁵)

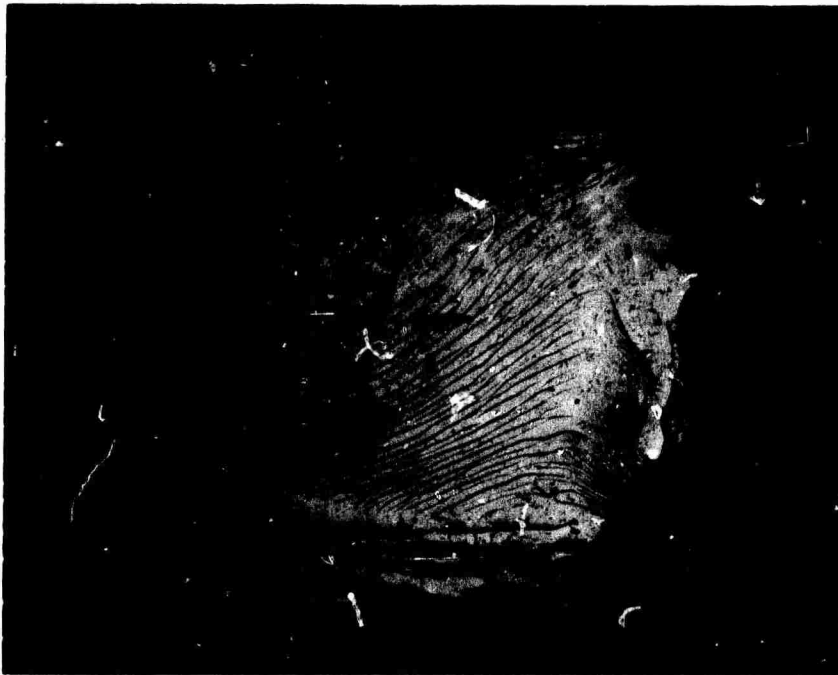


Figure II-3. This is an example of dendritic growth, growth No. 32, that arises from fast growth rates around the edges of the substrate. Note that the uneven surface features are terraces that have grown inwards from the dendrites. (111B, 8X)

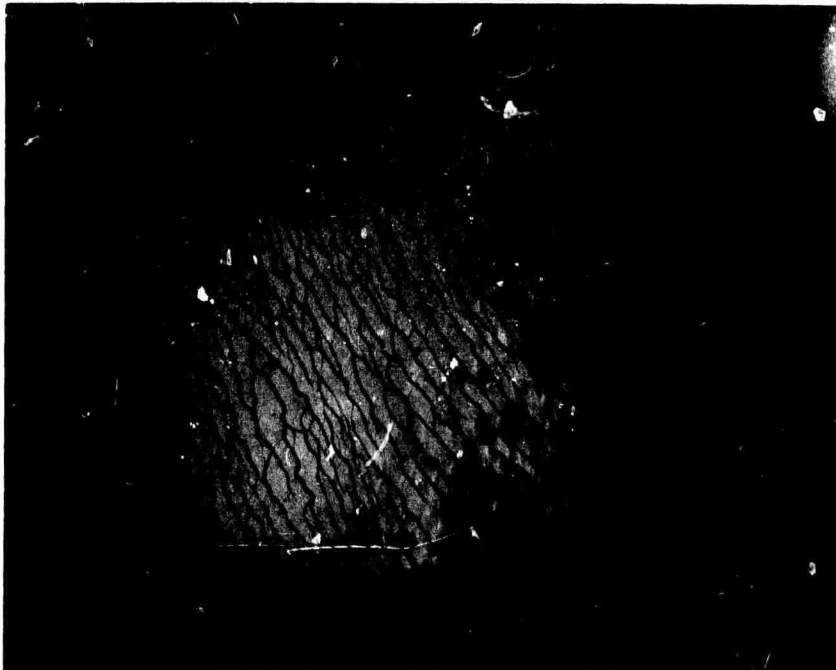


Figure II-4 a. Growth No. 38 was masked around the edges of the substrate with a carbon frame so that the growth would be essentially normal to the surface. (111B, 8X)



Figure II-4 b. Growth No. 62 was cooled at a faster rate so that the rate of growth normal to the surface would exceed transverse growth rates. Note that terracing occurs uniformly across the surface (100, 8X)

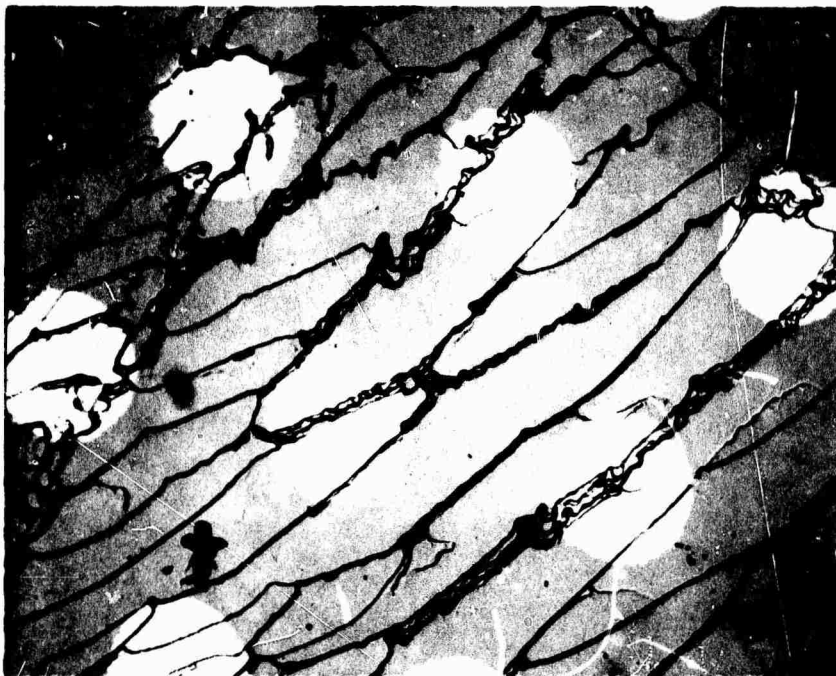


Figure II-5. Typical micrographs of terracing that show (a) the ragged steps found on (111) A surfaces, growth No. 66 (50X)



Figure II-5 b. The smooth sharp edges found on (111) B surfaces, growth No. 38 (50X)



Figure II-6. These growths show typical hillock shapes found for particular substrate orientations. (a) Triangular hillocks are found on (111) A surfaces growth No. 63. (10X)

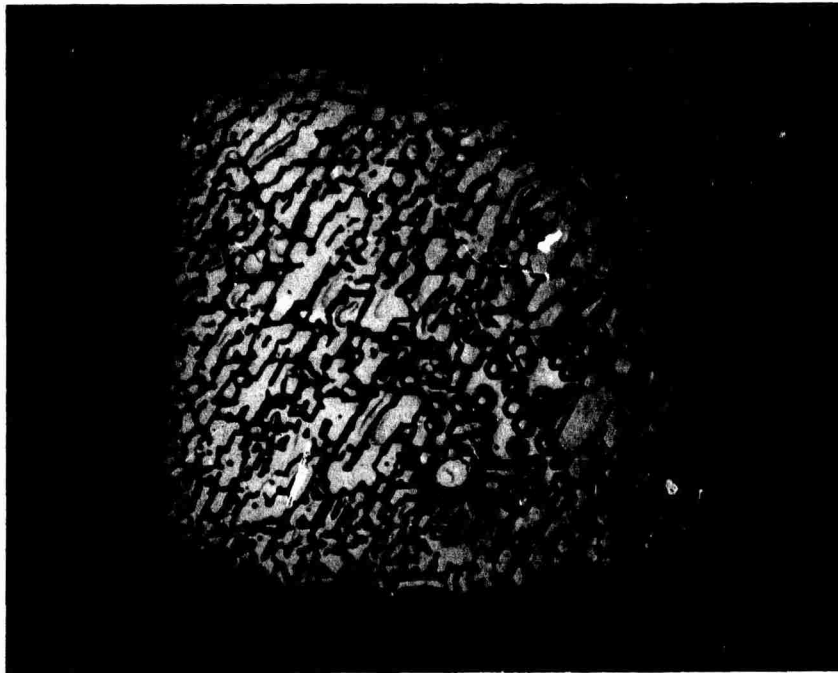


Figure II-6 b. Hexagonal hillocks are found on (111) B surfaces, growth No. 30 (8X)



Figure II-6 c. Rectangular hillocks are found on (100) B surfaces, growth No. 48 Note that when the hillocks coalesce in large numbers, a terracing pattern appears to form. (10X)

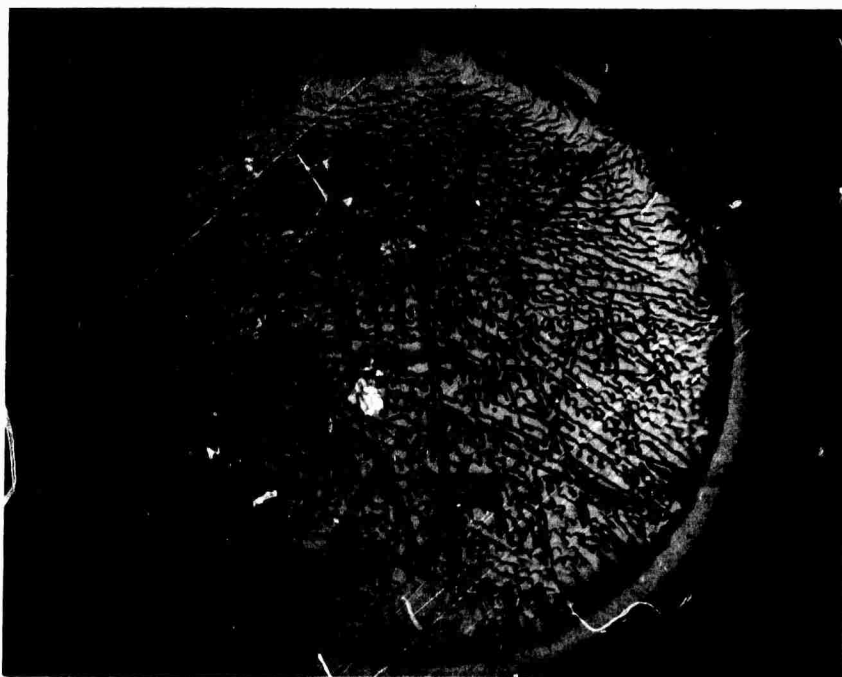


Figure II-7. This growth shows a correlation of some surface features with possible defects inadvertently introduced during the preparation of the substrate. Some of the terraces and long lines appear to extend inwards from scratches observed on the masked portion of the substrate. (111A, 12X)

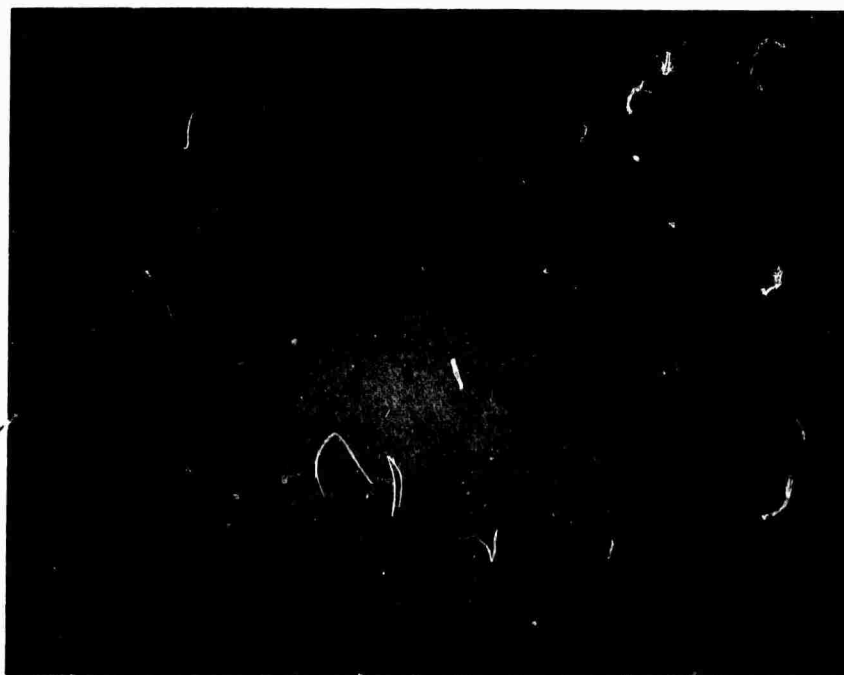


Figure II-8 a. The substrate was given a final rinse in acetone and a stain was left, growth No. 47. Note the propagation of the stain from the masked portion of the substrate into the growth. (100, 10X)

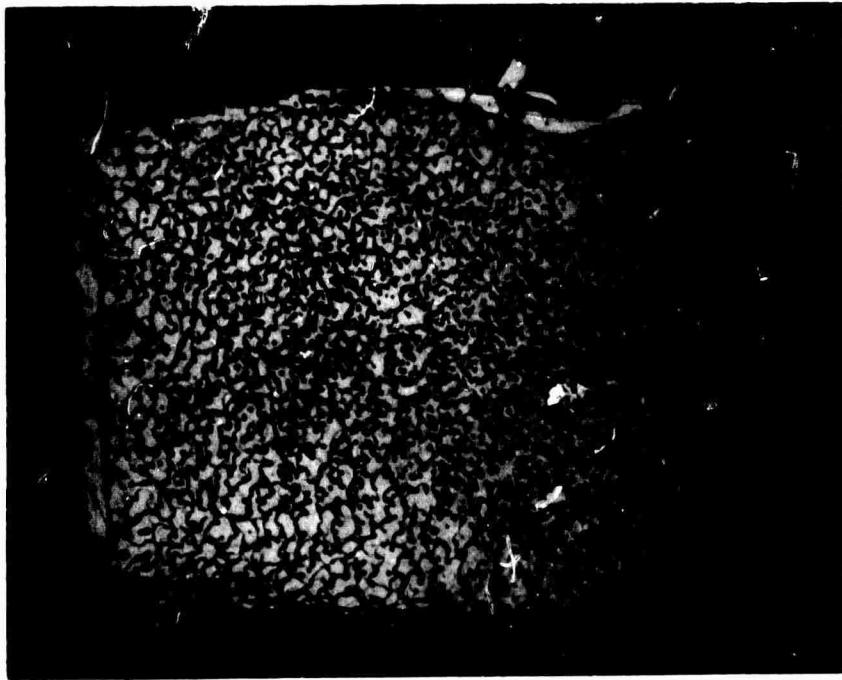


Figure II-8 b. The substrate was air-abraded with 50 μm particles prior to growth, growth No.34. Note the resultant irregular terracing and numerous holes (111B, 8X)

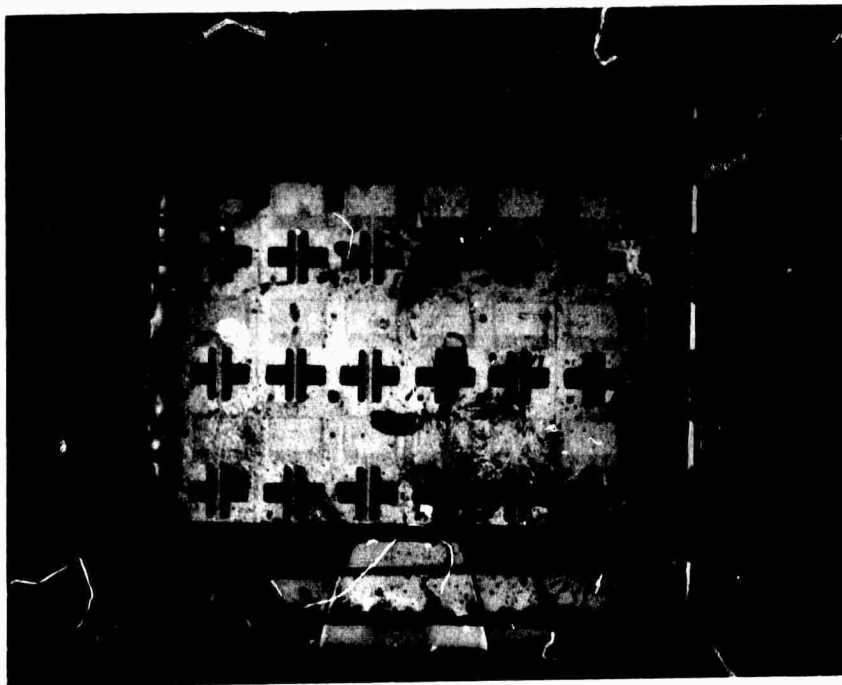


Figure II-10. Photodeposited F.E.T. networks on growth No. 47 (100, 10X)

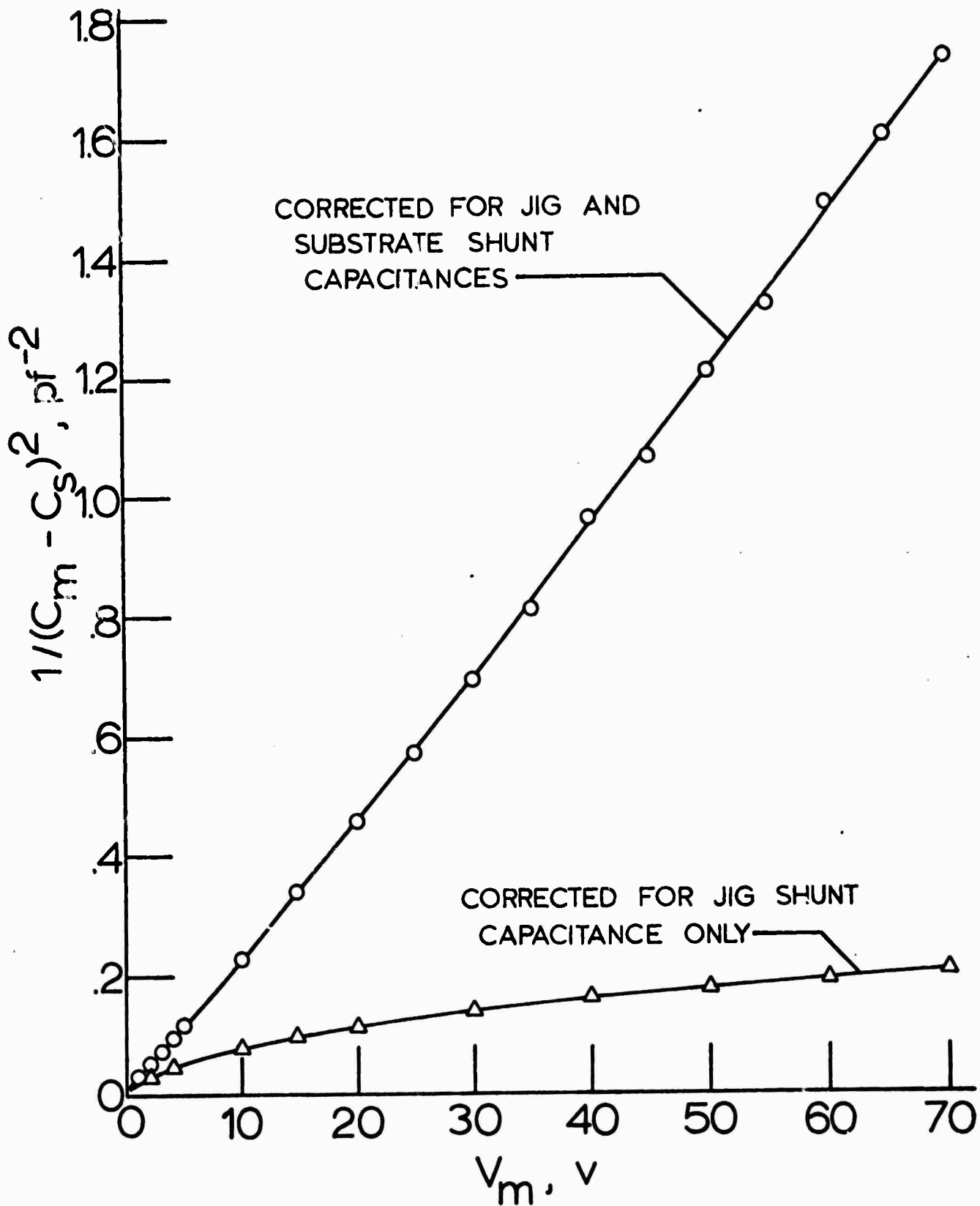


Figure II-9. Carrier density determination from Schottky barrier capacitance and bias voltage measurements. The slope gives $n = 2 \times 10^{14} \text{ cm}^{-3}$ for growth No. 38. The capacitance for an infinite bias voltage has been subtracted from the measured capacitance. This corrects for the jig, substrate and edge shunt capacitances.

III. APPLICATIONS OF COMPOUND SEMICONDUCTOR MATERIALS

A. Purpose of Work

The aim of this work is to utilize thin film epitaxial GaAs layers in the design and fabrication of microwave and acoustical devices. The devices of interest are planar devices with conduction along a thin film of GaAs deposited on a semi-insulating substrate. For this purpose, it is necessary to have high quality substrates as well as high quality semiconducting GaAs and considerable attention must be paid to the quality of the contacts used.

B. Progress to Date

We are interested in using these epitaxial layers in three kinds of devices: (1) a unilateral Gunn amplifier, (2) an improved GaAs FET amplifier, and (3) a surface acoustic wave amplifier. All three of these devices make use of epitaxial layers in the 10-30 μm range, with carrier densities typically 10^{14} - 10^{15} cm^{-3} and room temperature mobilities of 6000-8000 $\text{cm}^2\text{V}^{-1}\text{sec}^{-1}$. Common to all three of these projects is the problem of obtaining both good quality ohmic contacts to the material and Schottky-barrier or insulated-gate contacts for the control of space charge. Hence our first experiments with the liquid-phase epitaxial material produced here involved the examination of contacting methods.

a. Contacts, We have previously made contact to this material by regrowth using liquid epitaxy. There are difficulties, however, in obtaining very thin contacts with well-controlled size on planar surface oriented devices. If the contacts are too thick, any chemical etching which is made to define the contacts tends to undercut and thus the size of the contact is not well defined. We have therefore concentrated on alloyed contacts. Most of our work has been devoted to the study of Ge-Au contacts which have been fairly satisfactory in the past, providing the alloying time is kept short and the surface of the GaAs is kept extremely clean before contacting. The process involves the evaporation of a Ge-Au alloy onto the GaAs surface with subsequent short alloying times of the order of 30 secs-1 minute. Originally, the samples were chemically cleaned, the evaporation of the Ge-Au carried out in a vacuum chamber, and the samples then removed and alloying

undertaken in a hydrogen furnace. This system has the disadvantage that chemical cleaning tends to be imperfect; oxidation could occur after the time the sample was removed from the vacuum chamber. Alternatively, if alloying were carried out within the vacuum chamber, it would be difficult to keep the alloying time short enough because of the difficulty in cooling the substrate fast enough. We have therefore reconstructed the vacuum chamber with the following modifications: (1) provisions to rf sputter-clean the sample in a pure Argon atmosphere, (2) a provision for rapidly cooling the substrate holder with cold water piped into it from outside the chamber, and (3) instrumentation to obtain good control over the temperature of the substrate at any time. With the new vacuum system in operation, we were able to obtain satisfactory contacts, as measured by the shape of the I-V characteristic to material, with a density of $5 \times 10^{14} \text{ cm}^{-3}$ grown by liquid epitaxy. It has been the experience in the past, as it was here, that Ge-Au contacts are more difficult to make to material grown by liquid epitaxy than by vapor epitaxy. This is presumably because of the lower trap density in material grown by liquid epitaxy. Our recent experience tends to confirm this, for although the contacts would seem to be useable in devices, it is apparent from the nature of the I-V characteristic that they are not yet as perfect as we would desire. Efforts are proceeding with changes in alloying time etc. to improve these contacts. However, for our present device applications we circumvent this difficulty by using contacts which are thicker or wider than the active GaAs layer.

A second problem arose with the material grown by liquid epitaxy due to terracing of the surface in the growth process. We were concerned at first that the effect of the terracing would be to give difficulties with masking and with the quality of the contacts. However, the depth of terracing ($< 1 \mu\text{m}$) seems to be such as not to give any serious difficulties in our present configuration.

As it appears now, our future requirements will include thinner layers of 1-10 μm having improved surface flatness and better quality contacts. In both these cases the reduction or elimination of the

terracing features would probably be advantageous.

b. GaAs Unilateral Gunn Amplifier and FET Amplifier: The configuration of the GaAs unilateral amplifier is shown in Fig. III-1. The amplifier is essentially a FET transistor. The gate gives control of the dc operation of the device and acts as a shield for the rf signal, reducing the direct coupling between input and output. The preparation of the samples is done following an integrated circuit technique that we developed in our laboratory for this purpose. The procedure we follow consists of three basic steps: high vacuum deposition of a Ge-Au layer for making ohmic contacts to the material; the deposition of an insulating layer of SiO_2 by a sputtering process; and the vacuum deposition of an Al layer to form the gate. At each step, the pattern of the layer is properly shaped depositing photoresist on top, exposing it through a mask and etching away selectively the unwanted materials. Using this FET configuration, we have made up to 50 Gunn amplifiers at a time. We have been using material of the order of 15 μm thick, with diode lengths varying between 20 μm and 100 μm and gate lengths 8 μm shorter than the diode length between contacts. The samples were tested by looking at the shape of the I-V characteristic. Their behaviour was satisfactory, fairly linear at low voltage, then saturating and breaking into oscillations at higher voltage. Initially there had been some worry because of work with earlier samples that there would be depletion of the GaAs near the insulating substrate because of electrons from the semiconductor going into traps in the insulating material. We had therefore chosen to use material somewhat thicker physically than we expected it to be electrically. As it turned out, the quality of the liquid epitaxial material used appears to be better than we had expected so that the electrical and physical thicknesses are comparable as far as we can tell. Consequently, the diodes did not operate properly as amplifiers. Instead most of them oscillated as Gunn oscillators, an unsatisfactory situation from the point of view of a device application. It did indicate however that the material is of good quality and suitable for use in planar Gunn devices. No difficulty was experienced with breakdown in the substrate, a problem which had occurred in earlier experiments. We are not absolutely certain why these difficulties are no longer present; however, it may be because a great deal more care has been taken with the preparation of the substrate and efforts have been made to eliminate damage to the substrate

surface in the present growth schedule.

It is intended to continue with the present application of the material to microwave devices, improving the efficiency and increasing the operating frequency. For this purpose we need material with a density in the $2 \times 10^{14} - 7 \times 10^{14} \text{ cm}^{-3}$ range, and a thickness of the order of 2-5 μm deposited on a high quality semi-insulating substrate. This material must be uniform, and have a smooth flat surface. Because the fields in Gunn devices are fairly high, there should be no difficulties with breakdown in the substrate. At the present time, the material being produced by liquid epitaxy is of the right density. It appears to be very uniform, but it is too thick. We can thin it down by at least a few μm as we have found in this Laboratory, by chemical etching. However, it would be desirable to have material somewhat thinner than the present material available to us. We intend to develop the contact technology further so as to make satisfactory contacts in Ge-Au. In a planar device, the contact size can be made larger in width than the width of the device itself so that minor difficulties with the contacts need not be too serious. In some devices we have made we have already done this, and found that devices will oscillate one way around where the contacts are smaller, and not the other way around when the contacts are larger. This is precisely what would be expected in such a configuration.

c. Acoustic Surface Wave Amplifiers and Delay Lines: We are also interested in the study of acoustic surface wave amplifiers and delay lines which use GaAs. The particular advantage of GaAs is that it is both piezo electric and that it possesses a high mobility. The latter feature makes GaAs very suitable to amplification of acoustic waves by the drifting carriers, since a strong interaction is obtained at relatively low electric fields. Typically these devices make use of a layer of GaAs approximately 10 μm thick deposited on the semi-insulating substrate. The density ranges from 10^{14} to 10^{15} cm^{-3} where the lower limit is fixed by the problem of making ohmic contacts to the material, while the upper limit comes about from damping of the acoustic waves by the electrons. The requirements of density and thickness are then quite comparable to those for the Gunn amplifier. The length of the device, however, is

much longer, typically of the order of 1 cm, since it is desired to generate delays which amount to about 3 μ s . It is the intention to extend the delay devices to a meanderline configuration on the layer so that very long delays can be obtained.

Experiments have already been carried out in this area to demonstrate the generation of acoustic delays on GaAs but so far only material grown by vapor epitaxy has been used. A schematic diagram of the delay device and the acoustic wave transducer are shown fig. III-2. The device has a novel type of transducer which relies on the excitation of surface waves by a FET structure. Delays of 2.5 μ s have been successfully produced and further investigation is in progress to improve the transducer conversion loss. Initial studies have also commenced on the use of the liquid epitaxy material for these devices and to date, it has been found that both ohmic contacts and Schottky-barriers can readily be manufactured on the material. The material presently produced in our Laboratory has, however, not been sufficiently long to construct acoustic devices since we are restricted by available masks in the photo-lithographic process. A later possibility in which we are very interested is to deposit a piezoelectric material such as CdS or ZnO on GaAs and use the much higher piezoelectric coupling coefficient of these materials to obtain larger acoustic gain as well as to make it possible to make efficient transducers to the acoustic surface wave on GaAs.

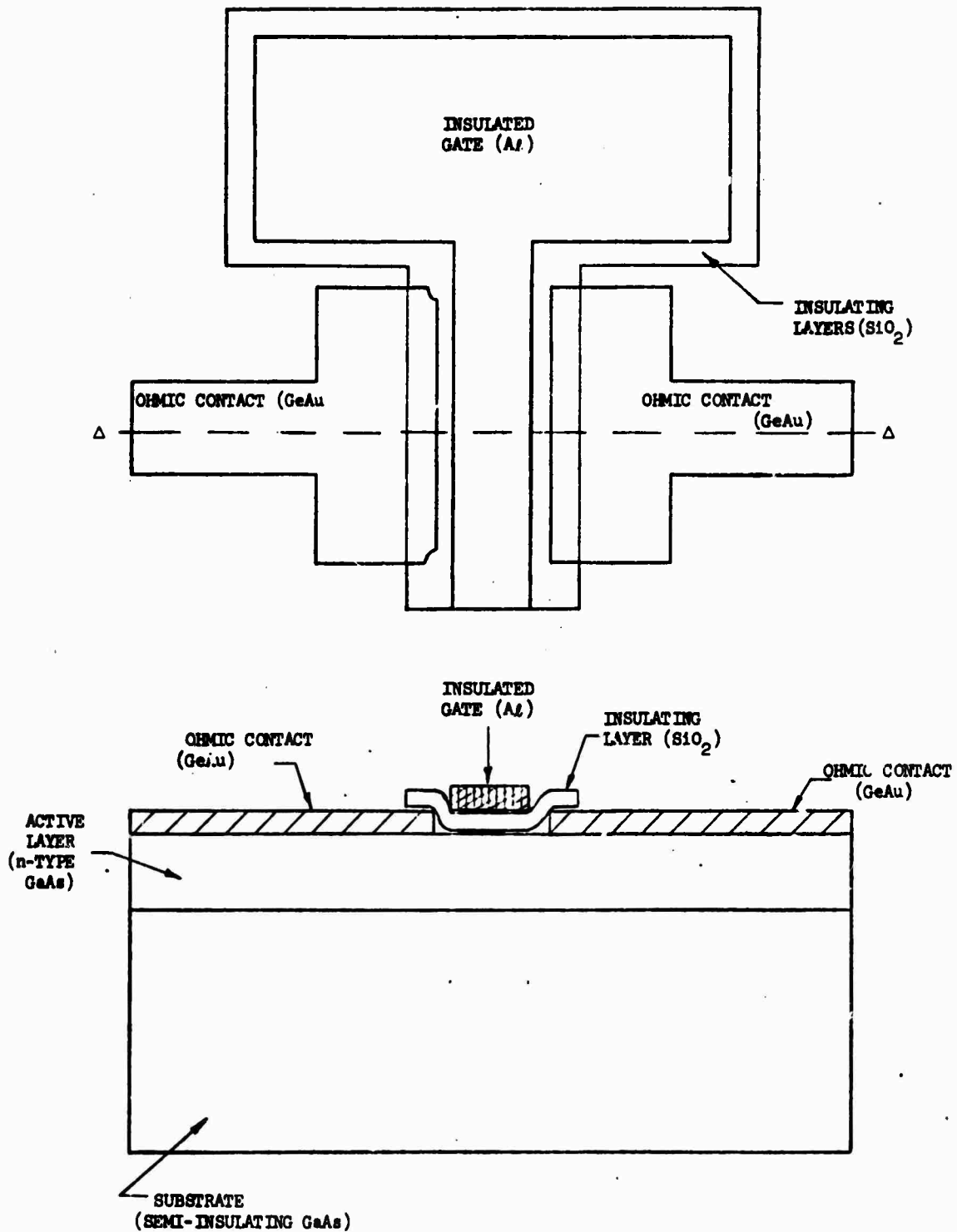


Figure III-1. Schematic diagram of a typical FET Gunn amplifier. Essentially similar configurations are used for both the unilateral amplifier and the more conventional FET amplifier.

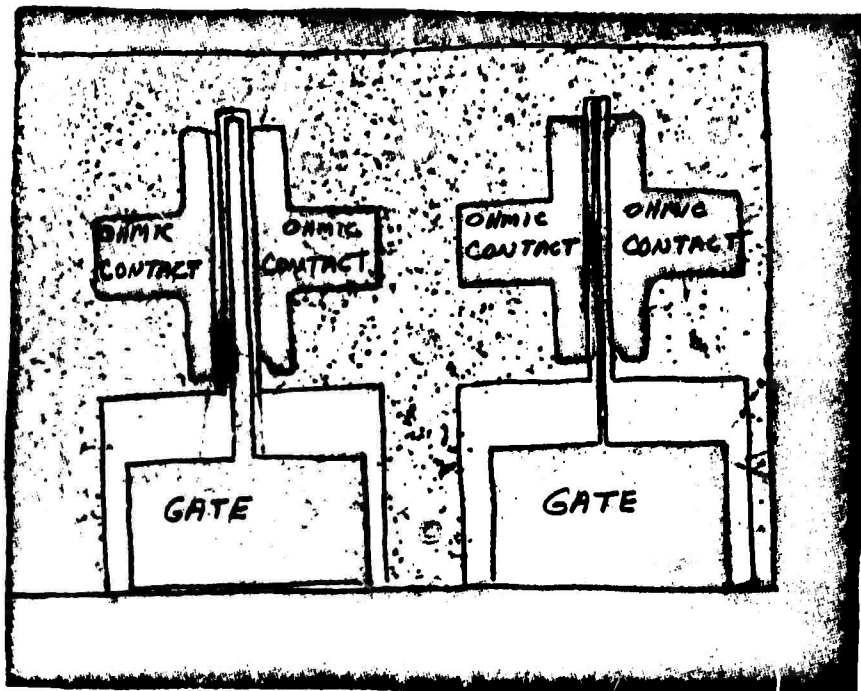
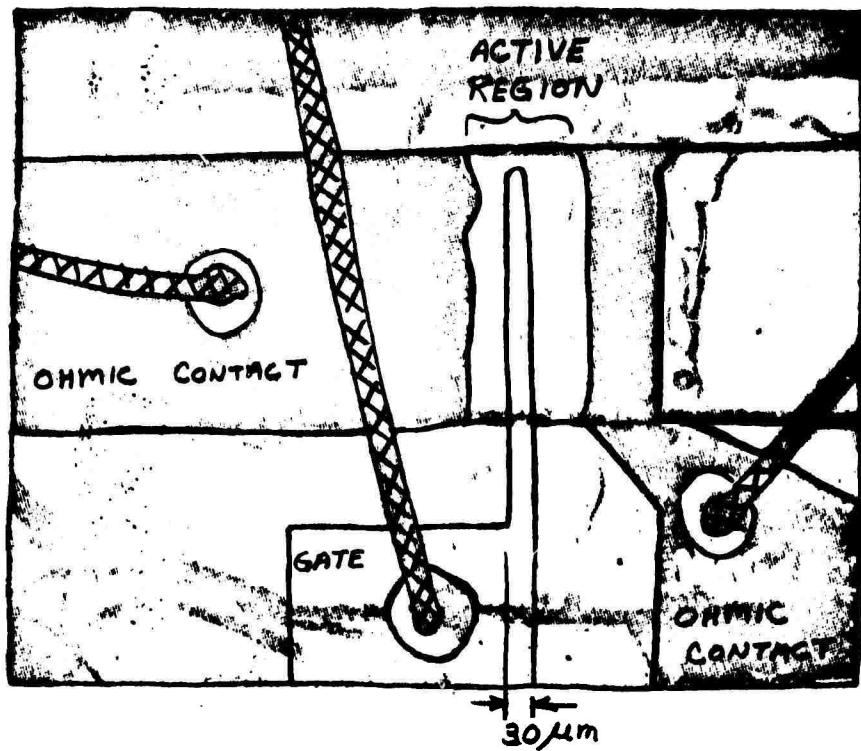


Fig. III-I-a. Photographs of FET Gunn amplifiers constructed using integrated circuit techniques.

☒ OHMIC CONTACTS ☒ AI - GATES

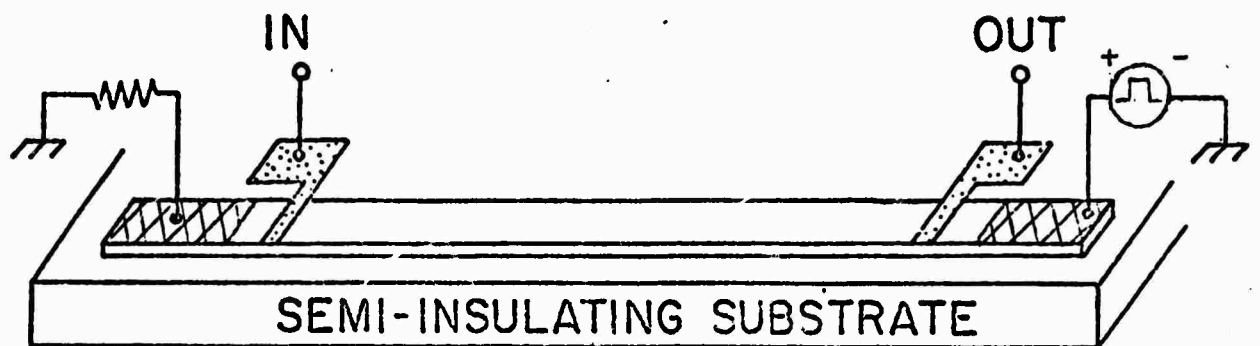


Figure III-2. Schematic diagram of a typical surface acoustic wave amplifier utilizing Schottky barrier transducers at each end of the device, the barrier being formed under the aluminum gate.

☒ OHMIC CONTACTS ☒ AI - GATES

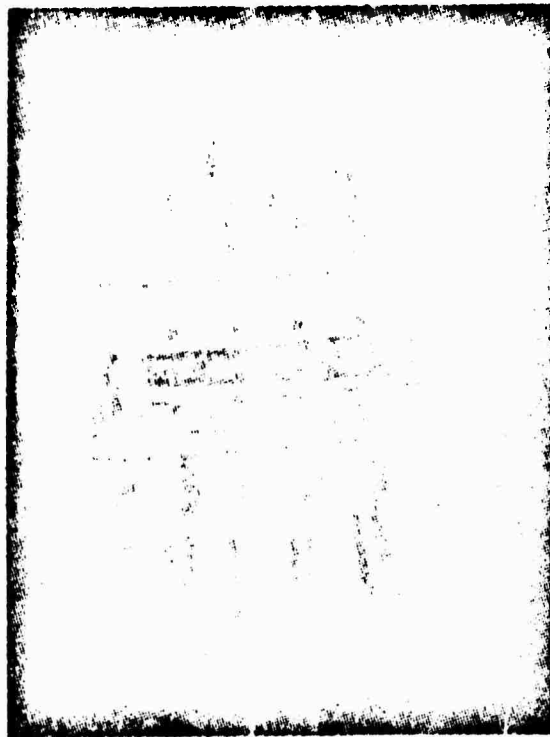
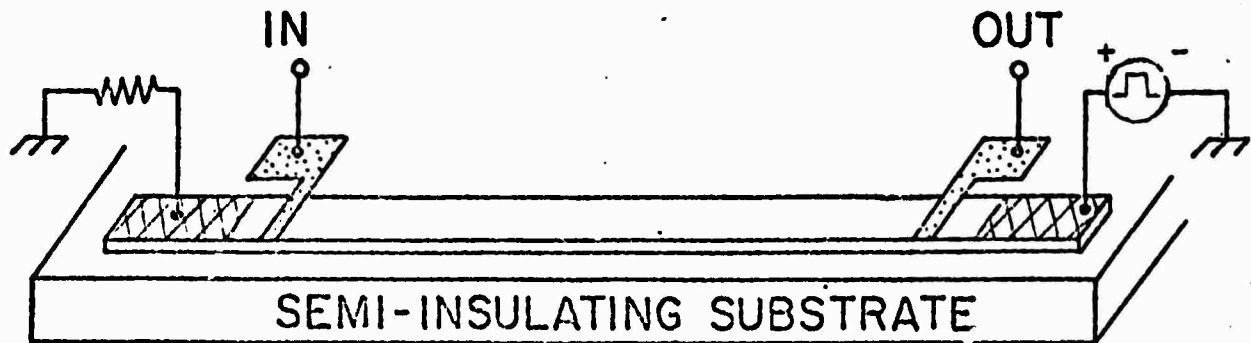


Figure III-2. Schematic diagram of a typical surface acoustic wave amplifier utilizing Schottky barrier transducers at each end of the device, the barrier being formed under the aluminum gate.

IV. RELATIONS BETWEEN DISLOCATIONS AND MECHANICAL PROPERTIES AND THE PRODUCTION AND CHARACTERIZATION OF DEFECT STRUCTURES IN COMPOUND SEMICONDUCTORS.

W.D. Nix and R. H. Bube*

A program of research is underway to devise techniques for modifying and characterizing the line defect structures in compound semiconductors through high temperature mechanical deformation. The purpose of this work is to develop a basic understanding of the effects of various types of dislocations and dislocation arrays on the important electrical and photoelectronic properties of compound semiconductors. At present our research is focused on the effects of deformation on the electronic structure and properties of GaAs as that system seems to have the most outstanding microwave device potential. It is anticipated that the results of this research will provide information which will contribute to either the microwave device research or the crystal growing effort.

Work to date has involved: (1) development of techniques for sample preparation; (2) the design and construction of a new 4-point bending device; and (3) the initial characterization of the electronic properties of undeformed GaAs single crystals. Following are summaries of the progress to date and the status of the research program.

* In our original proposal it was suggested that this program on effects of mechanical deformation be carried out by W.D. Nix and that R.H. Bube be associated with a related study involving electronic property measurements in compound semiconductors. It now seems appropriate to combine these parts of the program, and we are suggesting that they be combined into a single program directed jointly by Professors Nix and Bube. With this change, two students - Bruce Liebert (Nix) and Alice Lin (Bube) - are engaged in this part of the program. The research encompasses both the development of defect structures by mechanical deformation techniques and the appropriate electrical and optoelectronic measurements.

A. SAMPLE PREPARATION AND PRELIMINARY ELECTRONIC PROPERTY MEASUREMENTS

We have obtained two GaAs single crystal ingots with different purities and electrical properties from Bell and Howell Co. One ingot is an undoped n-type GaAs crystal with a carrier concentration of about $3 \times 10^{16} \text{ cm}^{-3}$ while the other is a semi-insulating Cr doped crystal with a room temperature conductivity of $5 \times 10^{-9} (\text{ohm-cm})^{-1}$. These ingots have been cut into samples of dimensions: length 20 mm, width 2 mm and thickness 2 mm with the orientation shown in Fig. IV-1. This particular

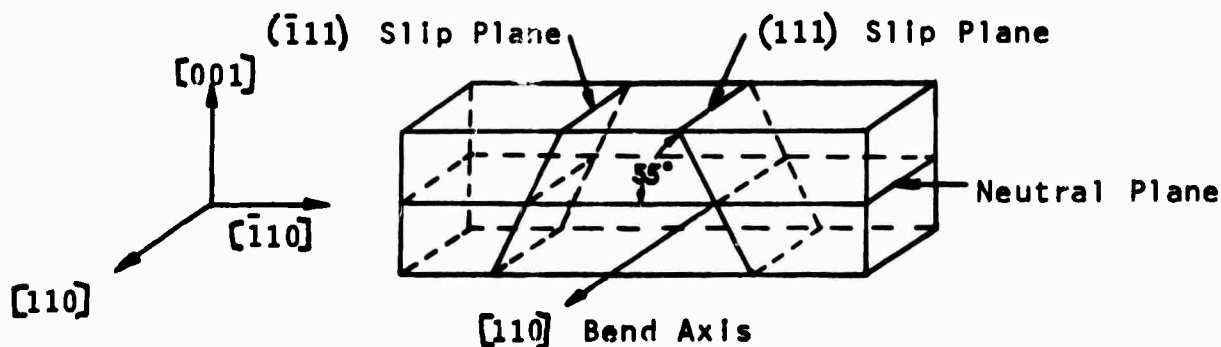


FIGURE IV-1. Sample Orientation for Bending

orientation has been chosen because the relation between excess dislocations of a given kind and the bending radius of curvature is unambiguous. By subjecting a crystal with this orientation to simple 4-point bending, only four different slip systems are activated and the Schmid factor is the same for each of these systems. Consequently the concentrations of excess dislocations on each of the four slip systems can be computed directly from the measured radius of curvature. This orientation was also chosen because it permits us to introduce either Ga dislocations or As dislocations, dependent on the bending sign¹. The geometry and mechanics of bending are discussed in more detail below.

The surface damage left by the cutting operations is removed by mechanically polishing with Linde A abrasive and the crystals are then etch-polished in a 5:100 (volume) solution of bromine in methanol for 5 minutes.

Our plan of attack with respect to each specific bending treatment is the following:

a. Measure the electrical properties of the sample before further treatment. Such measurements include the temperature dependence of dark conductivity and Hall effect, photoconductivity and photo-Hall effect, spectral response of photoconductivity, and thermally stimulated conductivity to give insight into the trap distribution.

b. Perform a bending experiment. Four-point bending at an elevated temperature is planned in order to achieve a constant radius of curvature over an appreciable length of the specimen. By maintaining constant temperature and deformation time, the load will be varied to introduce varying concentrations of line dislocations, with the radius of bending curvature and polarization of the bending face as the experimental parameters. During each bending experiment, a control sample will be subjected to the same atmosphere and temperature without bending.

c. Measure the electrical and photoelectronic properties listed in 1 above for the control sample and for the deformed sample.

At the present time, we are involved in the measurements that will define the properties of the undeformed samples of high-resistivity GaAs:Cr. The spectral response of photoconductivity at room temperature shows the expected maximum at 0.88 microns, as well as extrinsic photoconductivity extending out to 1.6 microns, i.e., excitation from levels near the center of the bandgap. Such a system should be a fairly sensitive detector for the addition of new imperfections through dislocations.

B. Mechanical deformation

As noted earlier, 4 point bending is being used to introduce dislocations into the GaAs crystals under study. The primary reason for using 4 point bending is that the mechanical moment in the center portion of the crystal beam is constant (position independent) and consequently the radius of curvature and dislocation density is expected to be constant. As shown in Fig. IV-2, the bending moment is Pb , where P is the half load and b is the distance

between the point of loading and the support.

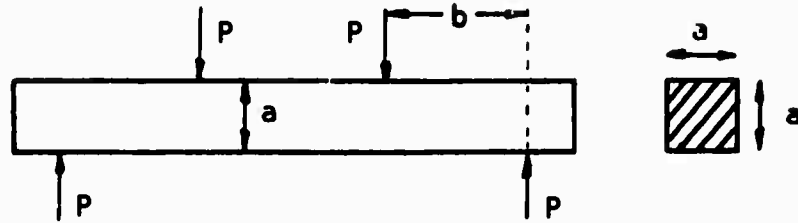


Figure IV-2. Four Point Bending

If τ is the critical resolved shear stress at which slip in the close packed directions on the octahedral planes occurs, it follows from geometry and the use of Schmid's law (crystal oriented as in Figure IV-1.) that the critical half load for plastic flow is

$$P_c = \frac{a^3 \tau}{3b} \sqrt{\frac{3}{2}}, \quad (1)$$

where a and b are the dimensions defined in Fig. One can estimate the high temperature shear strength of our n -type crystals from the literature.² The prediction is about 7000 psi at 500°C. Using this result in equation (1) and the geometry of our crystals, we find that half loads of a few pounds should be sufficient to produce plastic bending in a reasonable period of time.

One further comment about the bending geometry should be made. Simple bending of crystals, with the orientation of Fig. IV-1, will produce only 60° dislocations. The density of dislocations (from all four slip systems) is

$$\rho = \frac{2}{Rb \sqrt{3} \cos \alpha}$$

where α is defined in Fig. (1), R is the bending radius of curvature and b is the magnitude of the Burger's vector ($\frac{a_0}{\sqrt{2}}$, where a_0 is the lattice parameter, $a_0 = 5.65 \text{ \AA}$). For a radius of curvature of 10 cm, the excess dislocation density is $5 \times 10^6 \text{ cm}^{-2}$ and the concentration of dislocation sites

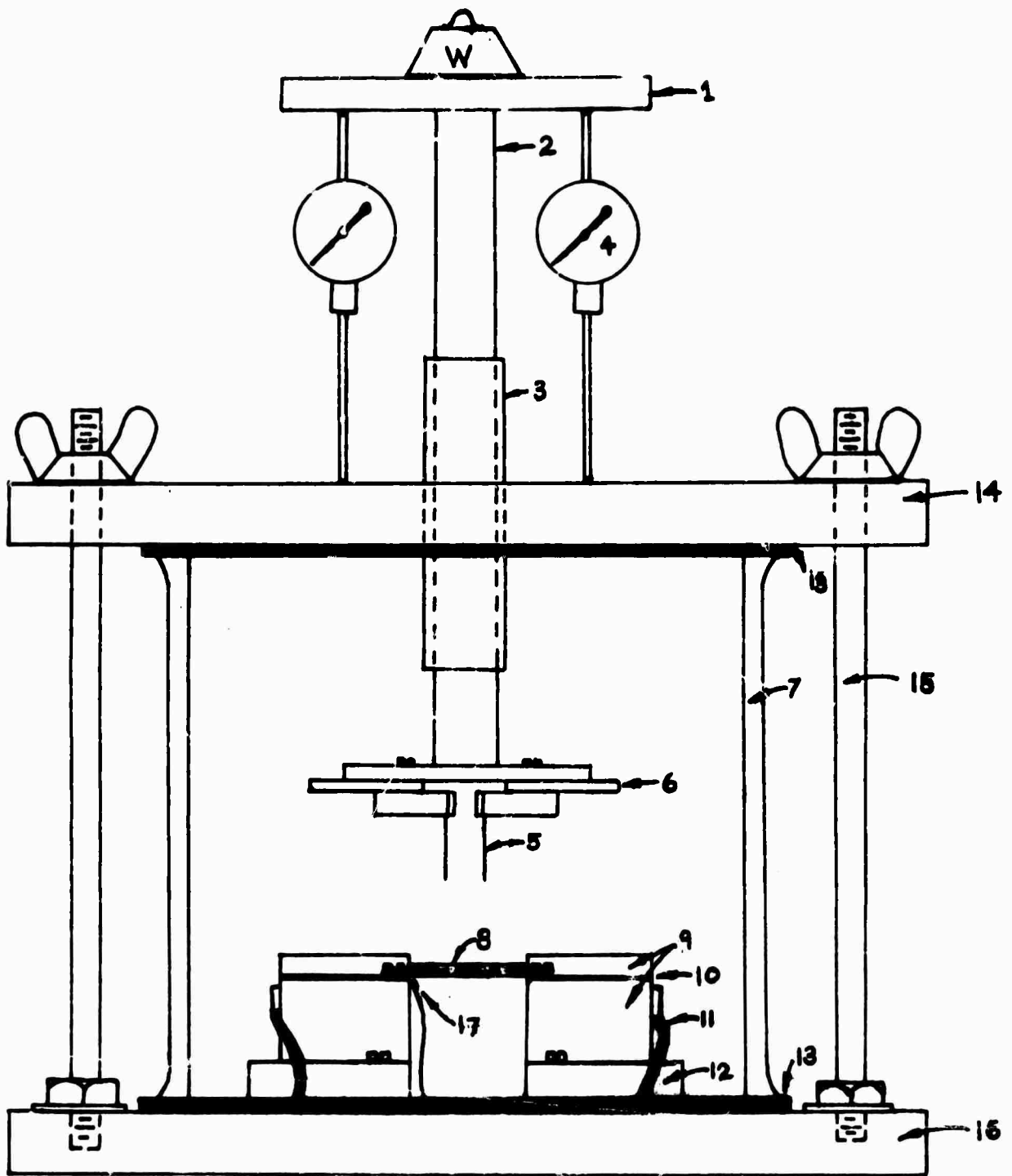
becomes $1.25 \times 10^{14} \text{ cm}^{-3}$.

A considerable amount of time has been spent designing, fabricating and modifying a bending apparatus of the Vogel type³, shown in Fig. IV-3, to be used with the high resistivity GaAs crystals. This design offers the advantage of heating, bending and cooling the sample in less than 30 seconds⁴. Most of the structural materials are phenolic, since it is stable, cheap and easy to machine. The actual apparatus is enclosed in a pyrex cylinder and an inert gas will be used to prevent unwanted reactions during high temperature bending.

The sample rests on two graphite blocks, covered with a thin sheet of molybdenum to provide a good electrical contact. Quartz was selected for the knife edges after the graphite was found to act as an effective heat sink, preventing the sample from deforming. Also, quartz is considerably harder and should not have to be replaced after each run. The amount of deflection is measured on two dial gauges to calculate the radius of curvature and to relate this to the density of dislocations. Temperature is measured with a chromel-alumel thermocouple located in the vicinity of bending. The adjustable base and knife edges allows samples from 10-50 mm to be accommodated.

REFERENCES

1. J.D. Venables and R.M. Broudy, J. Appl. Phys. 29, 1025 (1958).
2. N.P. Sazhin, M.G. Mil'vidskii, V.B. Osvenskii and O.G. Stolyarov, Sov. Phys. Solid State, 8, 1223 (1966).
3. F.L. Vogel, J. Metal, 946 (1956).
4. R.L. Petrusovich and E.S. Sollertinskaya, Sov. Phys. Crystallography, 9, 606 (1965).



FOUR POINT BENDING APPARATUS

- | | | |
|-----------------------|-------------------------|---------------------|
| 1. Platform | 7. Pyrex cylinder | 13. Neoprene gasket |
| 2. Plunger | 8. GaAs sample | 14. Lid |
| 3. Alignment tube | 9. Graphite blocks | 15. Support rod |
| 4. Dial indicator | 10. Molybdenum sheet | 16. Base |
| 5. Quartz knife edges | 11. Wire lead to variac | 17. Thermocouple |
| 6. Top platform | 12. Adjustable base | |

Figure IV-3.

V. ANNEALING AND PRECIPITATION STUDIES IN COMPOUND SEMICONDUCTORS

A program of research is underway to study the influence of post growth annealing upon the properties of crystals of compound semiconductors. Two key topics are under investigation: the equilibrium concentration of electrically active defects in these crystals for different conditions of temperature and component pressure; and the changes that occur in these crystals during cooling from annealing temperatures. The former topic involves the measurement of the Hall coefficient and the electrical conductivity of compound semiconducting crystals as a function of temperature and component pressure and the system under present study is the ZnTe:Al system. The latter topic involves the investigation of precipitation in compound semiconducting crystals, with the GaAs:Zn system under present study. It is anticipated that this work will provide valuable insight into the importance of post growth treatment of compound semiconducting crystals.

A. High Temperature Transport Measurements

The II-VI compound, ZnTe, is typical of the larger band gap II-VI compounds in its tendency to be one carrier type; ZnTe is always p type in its pure state and upon doping with donor impurities can be made n type only in a high resistivity state. Present theory relates this behavior to self compensation; donor dopants, such as aluminum or indium, are compensated by native acceptors, such as zinc vacancies in the case of ZnTe.

To obtain further insight into this problem, the high temperature defect equilibria of ZnTe:Al is under study by measurement of the Hall coefficient and the electrical conductivity as a function of temperature and component pressure. Several transport measurements have been made on ZnTe:Al above 350°C. The material was p-type with conductivity values ranging between 10^{-3} and 10^{-4} (ohm-cm)⁻¹ up to 600° C., at which temperature n-type behavior

appeared. The sample was subsequently cooled to 550°C. with retention of the n-type behavior.

Fig. V-1 illustrates the high temperature dependence of conductivity on Zn vapor pressure, in log-log form. Several features of these measurements are worth noting; 1) The conductivity is low resistivity n-type between 700°C. and 925°C. and pressures ranging from 10 to 400 Torr; 2) The slopes of the line segments for the lower temperatures are positive, and as the temperature is increased there is a decrease of slope at lower pressures, until finally, at the highest temperatures, a minimum with change in slope sign is observed 3) The sample came to equilibrium very rapidly, within a minute, after a change in temperature or pressure at all temperatures.

In Fig. V-2 is shown the Hall mobility as a function of the Zn vapor pressure at the various temperatures. In spite of the uncertainty of some of the data points, a pressure dependence of the mobility is apparent. The analysis and interpretation of these data is currently in progress.

B. Precipitation in Compound Semiconductors

The subject of precipitation in compound semiconducting crystals is intimately related to the question of impurity and native defect concentrations in the crystals since precipitation during annealing or cooling from annealing temperatures will change the concentration of these defects. Instances of precipitation with consequent degradation of electrical properties have been reported in a number of semiconductor systems. Among the III-V compounds, most studies have focused on GaAs because of its practical applications.

The initial activity has involved the examination of GaAs crystals, Zn doped from a Ga rich melt under varying growth conditions. Voids were present in most of the (111) platelets which formed, but to a lesser degree in those grown by cooling from 800°C. rather than 1000°C. Infrared transmission microscopy showed the crystals to be predominantly transparent, but the voids introduced some doubt and made any definitive analysis impossible.

Three GaAs crystals were then Zn-doped by vapor diffusion at 850° C. for three hours in an evacuated ampoule using a pure Zn source. Two of the crystals had been previously melt-doped and one was the pure bulk material. All three crystals proved to be completely opaque to infrared, which strongly suggests precipitation or pre-precipitation, but this is not conclusive evidence. These crystals are currently being examined for defect structures by x-ray topography, which, because of its nondestructive nature, must be done before the electron microscopy.

While the vapor diffusions and subsequent analyses were being performed, procedures were developed for analysis by electron microscopy using pure GaAs. Since the ultrasonic cutting device generates defects in the material, an abrasive type tool was made for cutting 1/8 inch diameter discs necessary for electron microscopy. Several etchants reported in the literature were tested on GaAs, but only $H_2SO_4:H_2O_2$ (30% SOLN) in a ratio of 16:1 was found to give the best combination of polish quality, rate, and reproducibility. A jet polisher, normally used for electropolishing of metal specimens, was adapted for use on GaAs, and has been used to produce several specimens for the electron microscope.

Upon completion of the x-ray topographic work, the vapor diffused samples will be examined in the electron microscope and, if the precipitates have developed to a large enough size, they will be identified by selected area diffraction. In any case, another series of GaAs samples will be Zn-doped from the vapor for varying lengths of time, different temperatures, and with different sources of doping material. This time the samples will be suitable for electrical measurements (such as Hall coefficients, resistivity, and optical absorption) which will be correlated with features observed in the x-ray topography and electron microscopy. Emphasis will be placed on cooling rate, with attempts being made to quench-in the high temperature structure. Initial investigative runs will also be started with Cd and Sn as dopants.

VI Scientific Aspects of Semiconductor Crystal Preparation

Interfacial Phenomena at the Solid-Liquid Interface in the Ga-As System: Determination of the Interatomic Potential Functions.

The interatomic potential functions for the Ga-As system have been determined by two different methods, (i) a simple parametric method and (ii) a more rigorous method.

It is essential to understand the individual contributions due to the covalent, ionic, metallic and dispersive interactions between the atoms in the solid and the liquid phases. At first, average interatomic potential functions for the system were constructed by the parametric method. The Morse potential function form was selected,

$$\phi = \phi^{\circ} \{ e^{-2\alpha(r-r_0)} - 2e^{-\alpha(r-r_0)} \}$$

where

ϕ = potential energy between two atoms

ϕ° = dissociation energy

α = shape parameter

r_0 = equilibrium spacing

r = distance between two atoms.

The three adjustable parameters, ϕ° , α and r_0 , in the potential function were determined from the macroscopic properties of Ga-As systems, such as the atomization energy, compressibility and data on the equilibrium structures. The parameters that were determined are shown in the following Table.

Type of atomic interaction	ϕ°	α	r_0
long range Ga-Ga	0.4384 e.v.	1.290 A ⁻¹	2.6512 A ⁰
long range As-As	0.1314 e.v.	0.759 A ⁻¹	2.6347 A ⁰
long range Ga-As	0.2401 e.v.	1.025 A ⁻¹	2.6430 A ⁰
short range Ga-As	3.0850 e.v.	1.150 A ⁻¹	2.4850 A ⁰

These parameters could be used for a crude approximation of the interfacial energies of the system in the future.

More refined potential functions for the GaAs crystal have been determined by the following method. The ionic interaction terms were evaluated by the formal standard calculations for the coulombic interaction energy using the proper effective charges of Ga and As atoms in the crystal. The dispersion terms were calculated by the London dispersion formula using reasonable experimental data on the polarizabilities and the ionization potentials. The short-range interaction terms were determined by applying the parametric method. (Morse potential) The potential functions that were determined are:

(i) The coulombic interaction term

$$\phi = \pm \frac{3.31776}{r^6} \quad (\text{e.v.}) ,$$

where r is in Å and positive for the interaction between atoms of the same kind and negative for interaction between atoms of different kind.

(ii) The dispersive interaction terms

$$\phi = - \frac{2.60}{r^6} \quad (\text{e.v.}) \text{ for the Ga-Ga interaction}$$

$$\phi = - \frac{445.6}{r^6} \quad (\text{e.v.}) \text{ for the As-As interaction ,}$$

$$\phi = - \frac{31.79}{r^6} \quad (\text{e.v.}) \text{ for the Ga-As interaction ,}$$

where r is in Å .

(iii) The covalent attractive interaction term

$$\phi = - 1.474 \exp (-1.902 (r-2.5852)) \quad (\text{e.v.}) ,$$

where r is in Å.

A similar method could be used for more improved potential functions of the liquid phase for this system if the necessary data on the physical properties of the liquid were available. Since currently available data for the liquid are limited, some statistical thermodynamic method should be used. This problem is being solved by employing a quasi-chemical approach.

Proposed Future Work

Using the above developed information about the solid and liquid phases, the atomic structure and energetics of the solid-liquid interface will be determined. The atomic and electronic structure, enthalpy, entropy and free energy of the interface will be determined for GaAs solid, for a fixed composition of the bulk liquid with varying compositions of the liquid at the interface. By minimizing the system free energy, the equilibrium surface adsorption and surface energy will also be calculated. This will be repeated for various compositions of the bulk liquid.

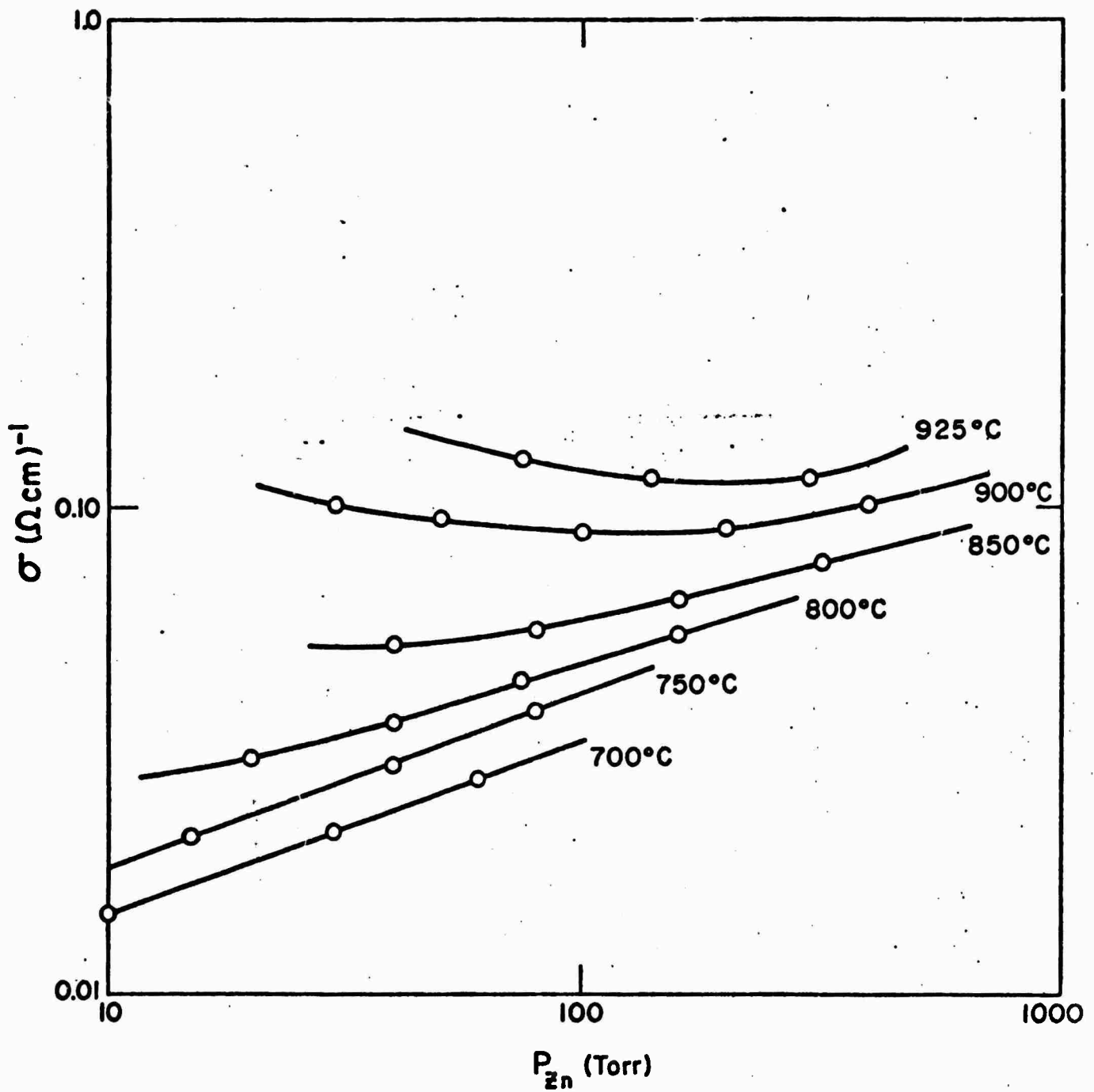


Figure V-1. The dependence of the equilibrium conductivity on Zn vapor pressure at fixed temperatures for Al doped ZnTe.

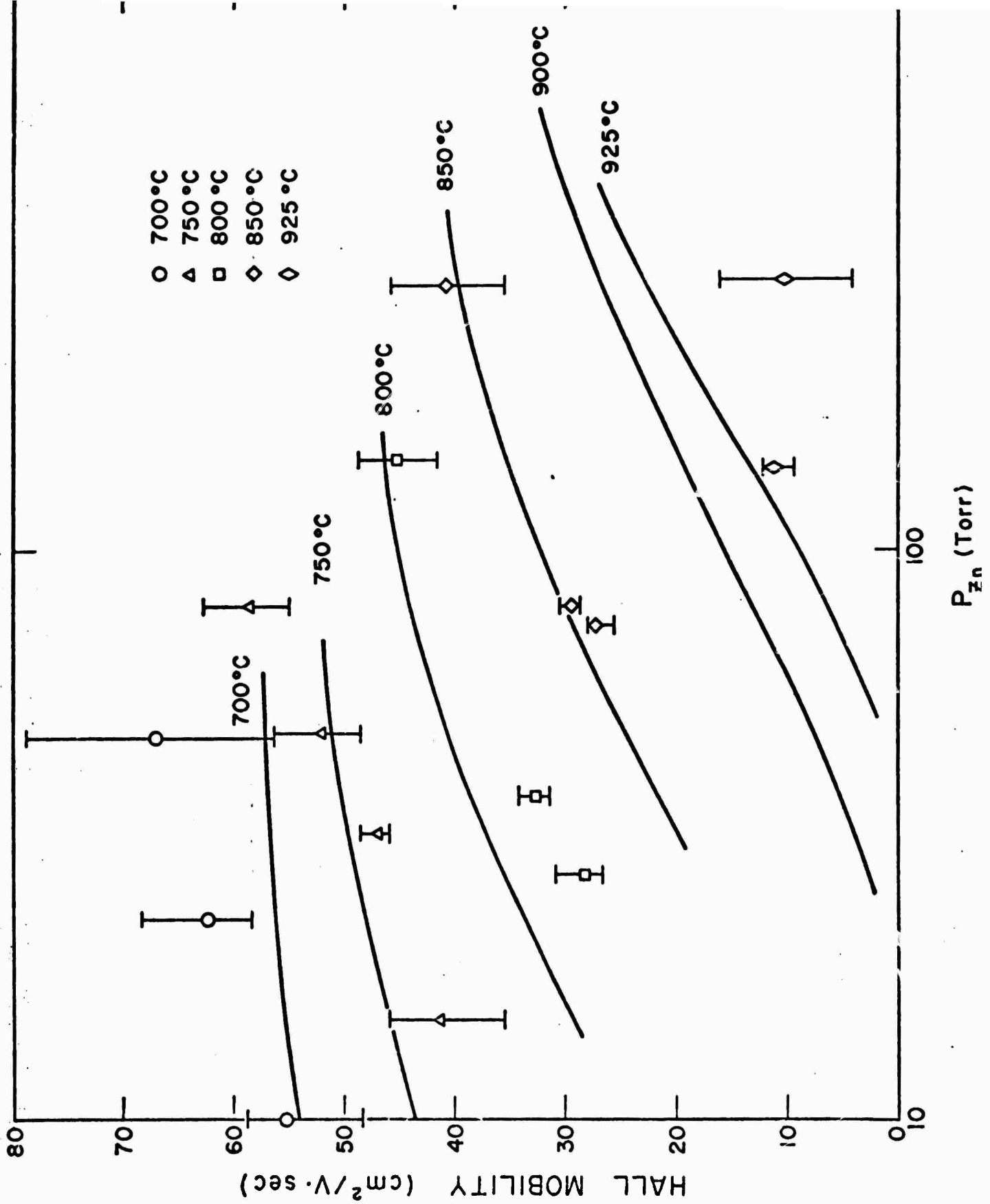


Figure V-2. The Hall mobility of Al-doped ZnTe as a function of Zn vapor pressure at fixed temperatures.